City of Morro Bay and
Cayucos Sanitary District

OFFSHORE MONITORING AND REPORTING PROGRAM

FIRST QUARTER RECEIVING–WATER SURVEY

MARCH 2016

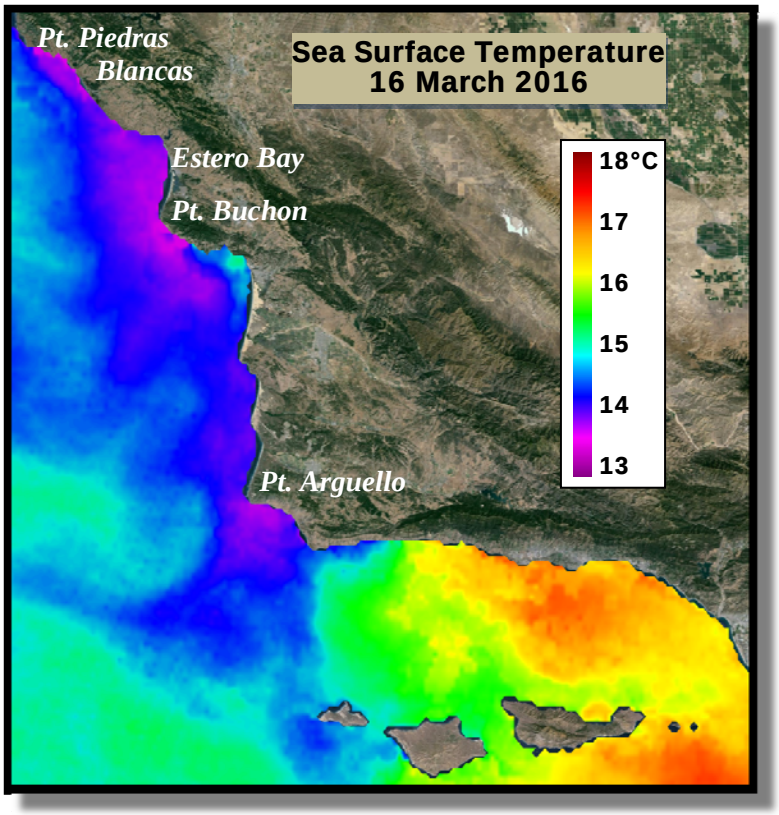

Marine Research Specialists
3140 Telegraph Rd., Suite A
Ventura, California 93003

Report to the

City of Morro Bay and Cayucos Sanitary District

955 Shasta Avenue
Morro Bay, California 93442
(805) 772-6272

OFFSHORE MONITORING AND REPORTING PROGRAM

FIRST QUARTER RECEIVING–WATER SURVEY

MARCH 2016

Prepared by

Douglas A. Coats

Marine Research Specialists

3140 Telegraph Rd., Suite A
Ventura, California 93003

Telephone: (805) 644-1180
Telefax: (805) 289-3935
E-mail: Marine@Rain.org

April 2016

marine research specialists
3140 Telegraph Road, Suite A • Ventura, CA 93003 • (805) 644-1180

Bruce Keogh
Wastewater Division Manager
City of Morro Bay
955 Shasta Avenue
Morro Bay, CA 93442

28 April 2016

Reference: Fourth Quarter Receiving-Water Survey Report – March 2016

Dear Mr. Keogh:

The attached report presents results from a quarterly receiving-water survey conducted on Thursday, 17 March 2016. The survey was conducted in accordance with the requirements of the NPDES permit issued to the City and District for discharge of treated wastewater to Estero Bay. The report evaluated compliance with permit limitations and assessed the effectiveness of effluent dispersion. Quantitative analyses of continuous instrumental measurements and qualitative visual observations confirm that the wastewater discharge complied with the receiving-water limitations specified in the permit, and with the objectives of the California Ocean Plan.

The offshore measurements confirmed that the diffuser structure and treatment plant continued to operate at a high level of performance. The measurements delineated a diffuse discharge plume containing low organic loads within a highly localized region northeast of the discharge point. Dilution within the plume exceeded expectations based on modeling and outfall design criteria.

Please contact the undersigned if you have questions regarding the attached report.

Sincerely,

Douglas A. Coats

Douglas A. Coats
Program Manager

I certify under penalty of law that this document and all attachments were prepared under my direction or supervision in accordance with a system designed to assure that qualified personnel properly gather and evaluate the information submitted. Based on my inquiry of the person or persons who manage the system, or those persons directly responsible for gathering the information, the information submitted is, to the best of my knowledge and belief, true, accurate, and complete. I am aware that there are significant penalties for submitting false information, including the possibility of fine and imprisonment for knowing violations.

Bruce Keogh

Mr. Bruce Keogh
Wastewater Division Manager
City of Morro Bay

Date April 29, 2016

TABLE OF CONTENTS

LIST OF FIGURES

LIST OF TABLES

INTRODUCTION

The City of Morro Bay and the Cayucos Sanitary District (MBCSD) jointly own the wastewater treatment plant operated by the City of Morro Bay. In March 1985, Region IX of the U.S. Environmental Protection Agency (USEPA) and the Central Coast California Regional Water Quality Control Board (RWQCB) issued the first National Pollutant Discharge Elimination System (NPDES) permit to the MBCSD. The permit incorporated partially modified secondary treatment requirements for the plant's ocean discharge. The permit has been re-issued three times, in March 1993 (RWQCB-USEPA 1993ab), December 1998 (RWQCB-USEPA 1998ab), and January 2009 (RWQCB-USEPA 2009). The March 2016 field survey described in this report was the twenty-ninth receiving-water survey conducted under the current permit.

The NPDES discharge permit requires seasonal monitoring of offshore receiving-water quality with quarterly surveys. This report summarizes the results of sampling conducted on 17 March 2016. Specifically, this first-quarter survey captured ambient oceanographic conditions along the central California coast during the winter season. The survey's measurements were used to assess the discharge's compliance with the objectives of the California Ocean Plan (COP) and the Central Coast Basin Plan (RWQCB 1994) as promulgated by the receiving-water limitations specified in the NPDES discharge permit.

The monitoring objectives were achieved by empirically evaluating tabulations of instrumental measurements and standard field observations. In addition to the traditional, vertical water-column profiles, instrumental measurements were used to generate horizontal maps from high-resolution data gathered by towing a CTD[1] instrument package repeatedly over the diffuser structure. This allowed for a more precise delineation of the plume's lateral extent.

SURVEY SETTING

The MBCSD treatment plant is located within the City of Morro Bay, which is situated along the central coast of California halfway between Los Angeles and San Francisco. Effluent is carried from the onshore treatment plant through a 1,450-m long outfall pipe, which terminates at a diffuser structure on the seafloor 827 m from the shoreline within Estero Bay (Figure 1). The diffuser structure extends an additional 52 m toward the northwest from the outfall terminus and consists of 34 ports that are hydraulically designed to create a turbulent ejection jet that rapidly mixes effluent with receiving seawater upon discharge. Currently, six of the diffuser ports are kept closed, thereby improving effluent dispersion by increasing the ejection velocity from the remaining 28 ports distributed along a 42-m section of the diffuser structure.

Following discharge from the diffuser ports, additional turbulent mixing occurs as the buoyant plume of dilute effluent ascends through the water column. Most of this buoyancy-induced mixing occurs within a zone of initial dilution (ZID), whose lateral reach in modeling studies extends 15.2 m from the centerline of the diffuser structure. Beyond the ZID, energetic waves, tides, and coastal currents within Estero Bay further disperse the dilute effluent within the open-ocean receiving waters. Both vertical hydrocasts and horizontal tow surveys are conducted around the diffuser structure to assess the efficacy of the diffuser, to define the lateral extent of the discharge plume, and to evaluate compliance with the NPDES permit limitations.

[1] Conductivity, temperature, and depth (CTD)

Figure 1. Location of the Receiving-Water Survey Area

Near the diffuser, prevailing flow generally follows bathymetric contours that parallel the north-south trend of the adjacent coastline. Because of the rapid initial mixing achieved within 15 m of the diffuser structure, impingement of unmixed effluent onto the adjacent coastline, 827 m away, is highly unlikely. Nevertheless, in the event of a failure in the treatment plant's disinfection system, collection and analysis of water samples at the eight surfzone-sampling stations shown in Figure 1 would be conducted to monitor for potential shoreline impacts. These surfzone samples would be analyzed for total and fecal coliform, and enterococcus bacterial densities.

Areas of special concern, such as the Morro Bay National Estuary and the Monterey Bay National Marine Sanctuary, are not affected by the discharge because they are even more distant from the outfall location. For example, the southern boundary of the Monterey Bay National Marine Sanctuary is located 38 km to the north, while the entrance to the Morro Bay National Estuary lies 2.8 km south. The southerly orientation of the mouth of the Bay, and the presence of Morro Rock 2 km to the south, serve to further limit seawater exchange between the discharge point and the Bay (Figure 1).

SAMPLING LOCATIONS

As shown in Figure 2, the offshore sampling pattern consists of six fixed offshore stations located within 100 m of the outfall diffuser structure. The red ⊙ symbols in the Figure indicate the target locations of the sampling stations (Table 1). The stations are situated at three distances relative to the center of the diffuser structure, and lie along a north-south axis at the same water depth (15.2 m) as the center of the diffuser. Depending on the direction of the local oceanic currents at the time of sampling, the discharge may influence one or more of these stations. The up-current stations on the opposite side of the diffuser then act as reference stations. Comparisons between the water properties at these antipodal stations quantify departures from ambient seawater properties caused by the discharge and allow compliance with the NPDES discharge permit to be determined.

The finite size of the diffuser is an important consideration in the assessment of wastewater dispersion close to the discharge. Although the discharge is considered a "*point source*" for modeling and regulatory purposes, it does not occur at a point of infinitesimal size. Instead, the discharge is distributed along a 42 m section of the seafloor, and, ultimately, the amount of wastewater dispersion at a given point in the water column is dictated by its distance from the closest diffuser port, rather than its distance from the center of the diffuser structure. This "*closest approach*" distance can be considerably less than the centerpoint distance normally cited in modeling studies.

Another important consideration for compliance evaluation is the ability to determine the actual location of the measurements. Discerning small spatial separations within the compact sampling pattern only became feasible after the advent of Differential Global Positioning Systems (DGPS). The accuracy of traditional navigation systems such as LORAN or standard GPS is typically ±15 m, a span equal to half the total width of the ZID itself. DGPS incorporates a second signal from a fixed, land-based beacon that continuously transmits position errors in standard GPS readings to the DGPS receiver onboard the survey vessel. Real-time correction for these position errors provides an extremely stable and accurate offshore navigational reading with position errors of no more than 2 m, and often of sub-meter accuracy.

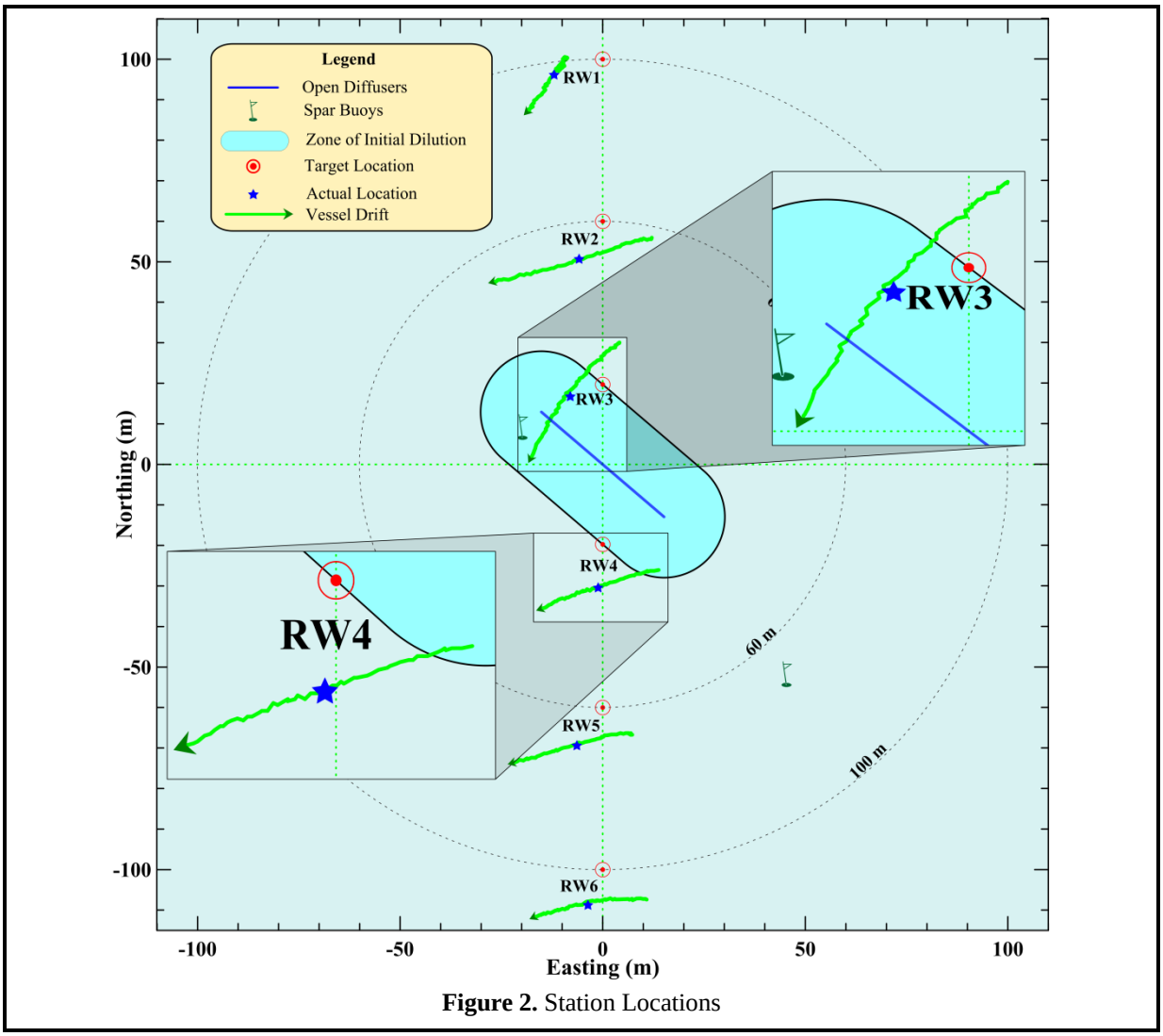

Figure 2. Station Locations

Table 1. Target Locations of the Receiving-Water Monitoring Stations

Station	Description	Latitude	Longitude	Center Distance[2] (m)	Closest Approach Distance[3] (m)
RW1	Upcoast Midfield	35° 23.253' N	120° 52.504' W	100	88.4
RW2	Upcoast Nearfield	35° 23.231' N	120° 52.504' W	60	49.4
RW3	Upcoast ZID	35° 23.210' N	120° 52.504' W	20	15.0
RW4	Downcoast ZID	35° 23.188' N	120° 52.504' W	20	15.0
RW5	Downcoast Nearfield	35° 23.167' N	120° 52.504' W	60	49.4
RW6	Downcoast Midfield	35° 23.145' N	120° 52.504' W	100	88.4

[2] Distance to the center of the open diffuser section
[3] Distance to the closest open diffuser port

During a diver survey in July 1998, the survey vessel's DGPS navigation system, consisting of a Furuno™ GPS 30 and FBX2 differential beacon receiver, was used to precisely determine the position of the open section of the diffuser structure (MRS 1998) and establish the target locations for the receiving-water monitoring stations shown in Figure 2 and listed in Table 1. Presently, the use of two independent DGPS receivers onboard the survey vessel allows access to two separate land-based beacons for navigational comparison, ensuring extremely accurate and uninterrupted navigational reports.

Recording of DGPS positions at one-second intervals allows precise determination of sampling locations throughout the vertical CTD profiling conducted at the six individual stations, as well as during the tow survey. Knowledge of the precise location of individual CTD measurements relative to the diffuser is critical for accurate interpretation of the water-property fields. During vertical-profile sampling, the actual measurement locations rarely coincide with the target coordinates listed in Table 1 because winds, waves, and currents induce unavoidable horizontal offsets (drift). Even during quiescent metocean[4] conditions, the residual momentum of the survey vessel as it approaches the target locations can create perceptible offsets. Using DGPS however, these offsets can be quantified, and the vessel location can be precisely tracked throughout sampling at each station.

The downcasts during the March 2016 survey were conducted progressing from south to north, beginning with Station RW6. The magnitude of the drift at each of the six stations during the March 2016 survey is apparent from the length of the green tracklines in Figure 2. The tracklines trace the horizontal movement of the CTD as it was lowered to the seafloor at each station. Their lengths and offsets from the target locations reflect the overall station-keeping ability during the March 2016 survey.

The time it took the CTD to traverse the water column to the seafloor, which averaged 1 min 25 s, was consistent among stations, as was the 30-m lateral distance traversed by the instrument package at all stations except Station RW1, where the CTD moved only 12.3 m (Figure 2). In contrast to the other stations, the vessel retained more of its northeastward momentum as it approached RW1, which limited the southwestward drift at the beginning of the downcast. This northeastward residual motion counteracted the influence of the moderate northeasterly breeze that prevailed at the time of the survey. Because of these higher-than-normal wind speeds, the lateral movement at the other stations was approximately three-times greater than the distance traveled by the CTD in most prior surveys. The lateral movement of the CTD movement at any given time is typically determined by a complex interplay between the external influences of winds and currents, and the vessel's residual momentum immediately prior to each downcast. However, the survey vessel's drift was probably dominated by the moderate breeze out of the northeast during the March survey.[5] Although the oceanic flow was also directed toward the southwest,[6] it probably contributed little to the lateral movement because surface vessels tend to be better sailors than drifters.

Regardless of the cause, detailed knowledge of the CTD's movement during downcasts is important for the interpretation of the water-quality measurements. Because the target locations for Stations RW3 and RW4 lie along the ZID boundary (red ⊙ symbols in the insets in Figure 2), knowledge of the CTD's location during the downcasts at those stations is especially important in the compliance evaluation. This is because the receiving-water limitations specified in the COP only apply to measurements recorded along or beyond the ZID boundary, where initial mixing is assumed complete. During the March 2016

[4] Meteorological and oceanographic conditions include winds, waves, tides, and currents.
[5] Refer to the meteorological and oceanographic observations listed in Table 4 later in this report.
[6] Refer to the drogued drifter track shown in Figure 3 later in this report.

survey, only the shallow portion[7] of the data collected at Station RW3 was subject to a compliance assessment because the cast began outside of the ZID and traversed the ZID boundary as it was transported to the southwest (see the upper right inset in Figure 2). In contrast, the CTD downcast at Station RW4 (lower left inset) began within the ZID, and crossed the ZID boundary shortly thereafter. Thus, only four shallow CTD measurements[8] were not subject to a compliance evaluation.

Compliance assessments notwithstanding, measurements acquired within the ZID lend valuable insight into the outfall's effectiveness at dispersing wastewater. For example, low dilution rates and concentrated effluent throughout the ZID would indicate potentially damaged or broken diffuser ports. Analysis of the outfall's operation over the past two and a half decades, however, demonstrates that it has maintained a high level of effectiveness in effluent dispersal. In fact, without the occasional measurements recorded within the ZID due to vessel drift, the extremely dilute discharge plume might remain undetected within all the vertical profiles collected during a given survey.

The data collected in the deeper portion of the downcast at Station RW3 was particularly valuable in that regard because the CTD passed directly over the diffuser structure as it approached the seafloor (see the CTD trajectory shown in green in the upper-right inset in Figure 2). When the CTD was 1.5 m above the seafloor, it encountered a wastewater ejection jet and captured mixing conditions shortly after discharge.

It has not always been possible to determine which measurements were subject to permit limits among hydrocasts near the ZID boundary, however. For example, prior to 1999 and before the advent of DGPS, CTD locations could not be determined with sufficient accuracy to establish whether the average station position was located within the ZID, much less how the CTD was moving laterally during the hydrocast. Because of these navigational limitations, sampling was presumed to occur at a single, imprecisely determined, horizontal location. Federal and state reporting of monitoring data still mandates identification of a single position for all of the CTD data collected at a particular station. Thus, for regulatory reporting, and for consistency with past surveys, the March 2016 survey also identifies a single sampling location for each station. These average station positions are identified by the blue stars in Figure 2, and are listed in Table 2 along with their distances from the diffuser structure.

Table 2. Average Position of Vertical Profiles during the March 2016 Survey

	Time (PDT)				Closest Approach	
Station	**Downcast**	**Upcast**	**Latitude**	**Longitude**	**Range[9](m)**	**Bearing[10](ºT)**
RW1	9:51:15	9:52:38	35° 23.251' N	120° 52.512' W	83.4	2
RW2	9:46:23	9:47:52	35° 23.226' N	120° 52.508' W	39.0	14
RW3	9:42:01	9:43:25	35° 23.208' N	120° 52.509' W	**7.6[11]**	41
RW4	9:37:09	9:38:32	35° 23.183' N	120° 52.505' W	**23.8[11]**	221
RW5	9:31:29	9:32:50	35° 23.162' N	120° 52.508' W	60.3	201
RW6	9:26:59	9:28:27	35° 23.140' N	120° 52.506' W	97.5	191

[7] Above 5.5 m
[8] Above 2.5 m
[9] Distance from the closest open diffuser port to the average profile location
[10] Angle measured clockwise relative to true north from the closest diffuser port to the average profile location
[11] Some of the CTD measurements were located within the ZID boundary (refer to the insets in Figure 2).

OCEANOGRAPHIC PROCESSES

The trajectory of a satellite-tracked drogued drifter measured oceanic flow throughout the March 2016 survey (Figure 3). Modeled after the curtain-shade design of Davis et al. (1982) and drogued at mid-depth (7 m), a drifter has been deployed during each of the quarterly water column surveys conducted over the past two decades. In this configuration, the oceanic flow field rather than surface wind dictates the drifter's trajectory, providing a good assessment of the plume's movement after discharge.

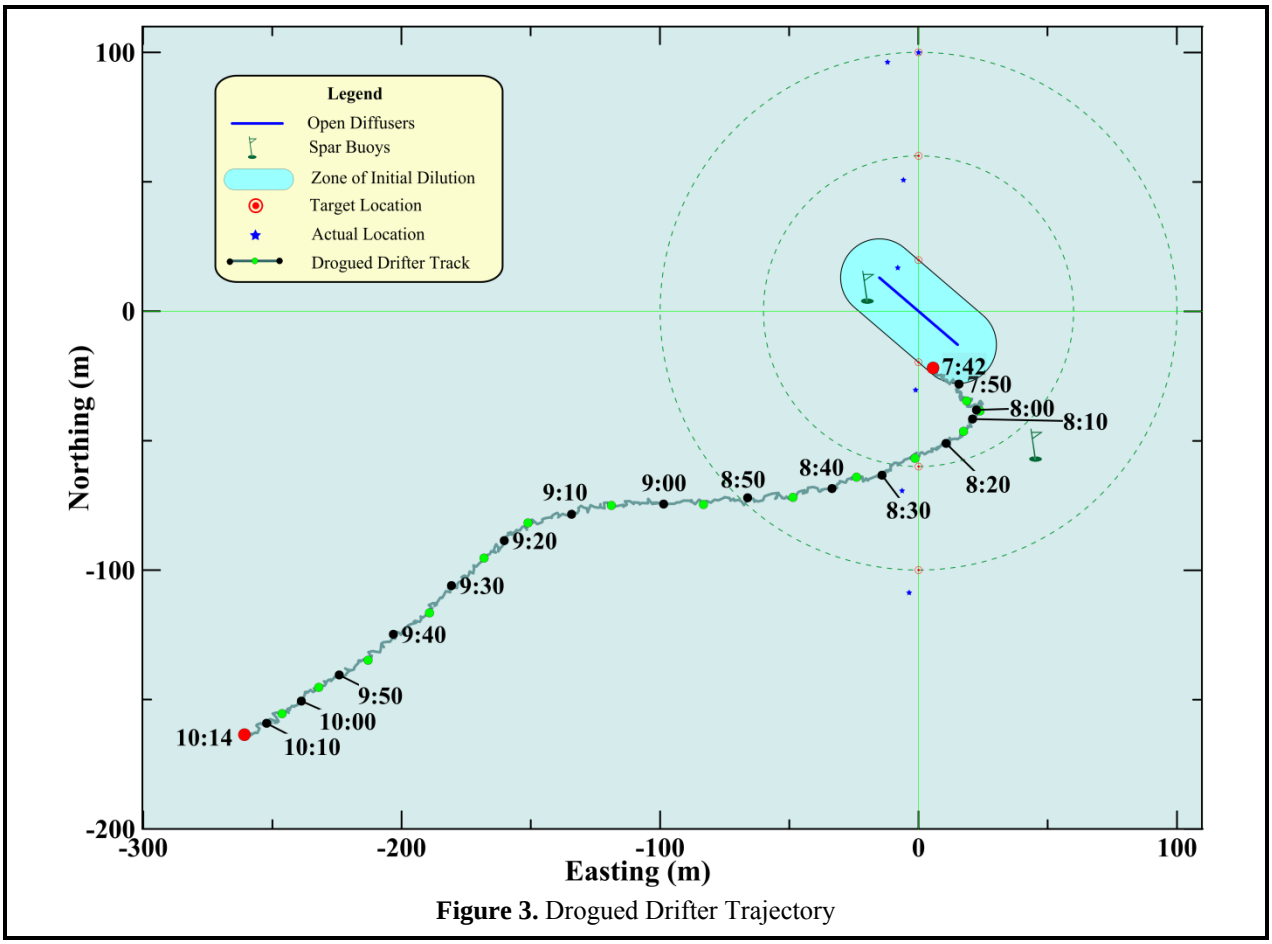

Figure 3. Drogued Drifter Trajectory

During the March 2016 survey, the drifter was deployed near the diffuser structure at 7:42 AM, and was recovered at 10:42 AM at a location 302 m southwest (242ºT[12]) of its original release point (red dots in Figure 3). However, in contrast to prior surveys, the drifter's trajectory was complex and inconsistent with the northeast location of the plume signature.[13] The complexity is reflected by three changes in direction and a slight reduction in speed near the end of the drifter's deployment. During the first 18 minutes, the drifter moved 24 m toward the southeast (131ºT) at a speed of 2.3 cm/s.[14] Between 8:00 AM and 8:10 AM, the drifter stalled, and then executed an unusual right-angle turn and began moving toward the southwest (257ºT) at a speed of 4.5 cm/s and along an arc that eventually led to near-westerly movement

[12] Direction measured clockwise relative to true (rather than magnetic) north
[13] See Figures 8 and 9 later in this report.
[14] 0.045 kt

after 8:40 AM. At 9:15 AM, the drifter began moving again toward the southwest (233ºT) at an average speed of 3.8 cm/s until it was retrieved an hour later. Shortly before its retrieval, its speed decreased as reflected by the closer spacing between the green and black dots in Figure 3, which show the drifter's progress at five- and ten-minute intervals.

At the average transport rate of 4.1 cm/s after 8:10 AM, effluent would have experienced a six-minute residence time within the ZID. However, the unusually complex drifter track did not accurately capture the movement of the effluent plume, which was found on the opposite (northeast) side of the diffuser structure. This was a highly abnormal occurrence, and indicated that the flow at the drifter's 7 m drogue depth did not determine the overall transport of the effluent plume. Instead, it is likely that a large amount of vertical shear was present in the flow field at the time of the survey, and that an opposing countercurrent, not captured by the drifter movement, was responsible for the plume's ultimate location in the upper water column.

Nevertheless, the overall flow direction measured by the drifter was consistent with the ebb tide that prevailed during the March 2016 survey (Figure 4). Ebb tides normally induce a weak southwestward (offshore) flow in the survey region. While tidal forcing may have contributed to the observed flow, currents within the survey area are often dominated by other processes, such as upwelling. Upwelling winds can also induce southwestward flow within the upper water column in response to northwesterly winds. Net wind-driven Ekman transport occurs at a 90º angle to the prevailing wind.[15] As a result, warm ocean waters within the surface mixed layer are driven offshore (southwestward) in response to the along-shore winds (toward the southeast). Near the coast, these warm surface waters are replaced by deep, cool, nutrient-rich waters that well up from below. The upwelled waters originate farther offshore and move shoreward along the seafloor as part of the upwelling process. Thus, upwelling can establish a strong vertical shear in the flow field within the survey area. The presence of upwelling-induced vertical countercurrents probably account for the aforementioned inconsistency between the weak and variable southwestward flow measured by the drifter within upper water column, and the observed northeastern location of the plume. The buoyant plume was probably carried rapidly toward the northeast by a strong undercurrent before it ascended into the upper water column where the weaker southwestward flow prevailed.

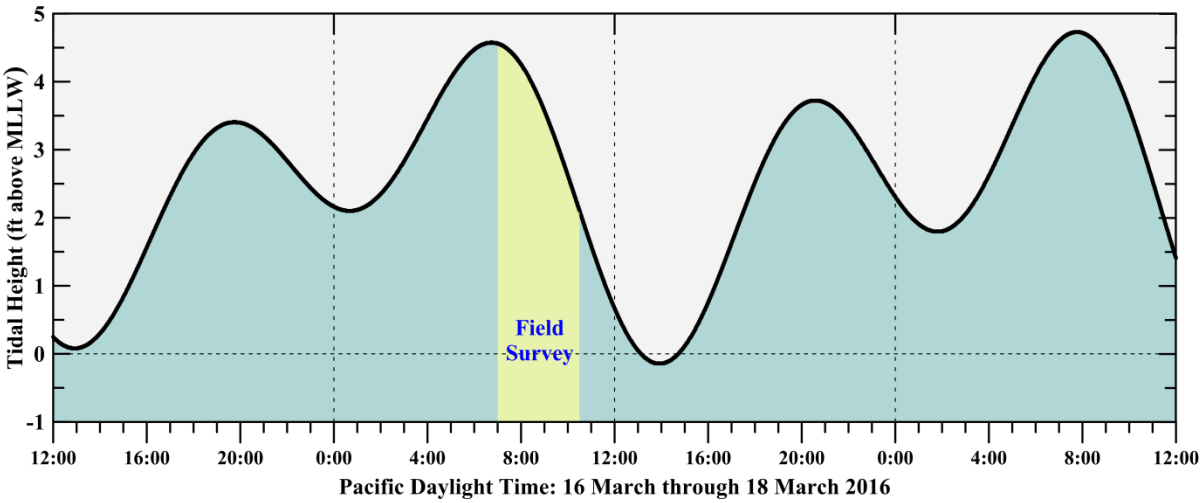

Figure 4. Tidal Level during the March 2016 Survey

[15] http://oceanmotion.org/html/background/upwelling-and-downwelling.htm

The onset of these upwelling-dominated processes begins with a rapid intensification of southeastward-directed winds along the central coast during late March and or early April as shown by the positive (blue) upwelling indices in Figure 5. This transition to more persistent southeastward winds is initiated by the stabilization of a high-pressure field over the northeastern Pacific Ocean. Clockwise winds around this pressure field drive prevailing northwesterly winds along the central California coast. The March 2016 survey was conducted during the onset of this spring transition.

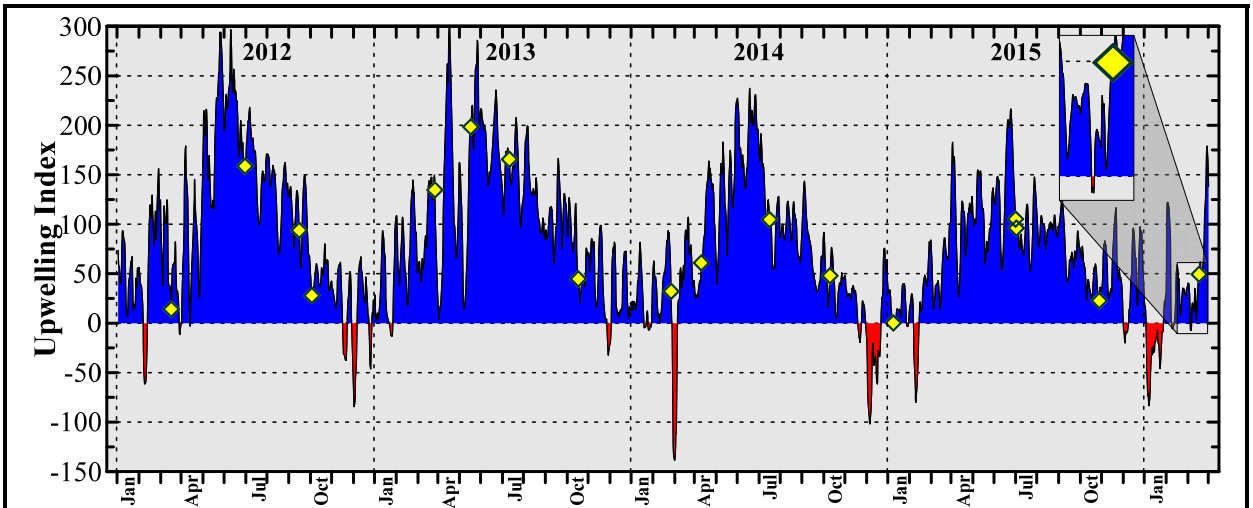

Figure 5. Five-Day Average Upwelling Index ($m^3/s/100$ m of coastline)

The nutrient-rich seawater that is brought to the sea surface near the coast by upwelling enables phytoplanktonic blooms that are the foundation of the productive marine fishery found along the central California coast. The vertical counterflow associated with persistent upwelling conditions also enhances vertical stratification of the water column. The influx of cold dense water at depth produces a shallow thermocline (<10 m) that is commonly maintained throughout summer and into fall.

Some degree of upwelling is almost always present during offshore surveys (yellow diamonds in Figure 5). During winter, upwelling is typically weak, and occasionally downwelling events, indicated by the negative (red shaded) indices in Figure 5, occur when passing storms temporarily reverse the normal wind pattern and drive surface waters shoreward. As the surface waters approach the coastline, they downwell, producing nearly uniform seawater properties throughout the water column.

Because the March 2016 survey took place at the very beginning of the spring transition, only moderate upwelling winds were present (see the inset showing the last yellow diamond in Figure 5). Nevertheless, these winds produced a pattern of sea surface temperatures indicative of upwelling processes within the central-coast region. This pattern was captured by the satellite image shown on the cover of this report. The image was recorded by infrared sensors on one of NOAA's polar orbiting satellites during a period of relatively cloudless skies on the day before the survey. Cooler upwelled water is visually apparent along the entire south-central coastline (purple and blue shading). Jets of upwelled water often extend offshore at major promontories, such as the one extending offshore Point Arguello at the time of the March 2016 survey. However, various swirls and eddies are also apparent in the surface temperature pattern, suggesting additional flow complexity. Thus, while the weak southwestward surface flow measured within northern Estero Bay during the survey is representative of either tidal or upwelling forcing, it is likely that other external oceanographic processes, such as large-scale along-shore pressure gradients, or

the passing of a large eddies embedded within the California Current also contributed to the surface flow pattern throughout the region.

Although the overall temperature distribution shown in the satellite image was consistent with upwelling, the 2ºC cross-shore contrast was somewhat smaller than the 5ºC difference seen during strong upwelling events. Thus, the March 2016 survey only captured the early stages of upwelling, and as a result, the water column was only moderately stratified. As described later in this report, the strength of the stratification was not sufficient to cause the buoyant plume to become trapped beneath the sea surface.

METHODS

The 38 ft F/V *Bonnie Marietta*, owned and operated by Captain Mark Tognazzini of Morro Bay, served as the survey vessel on Thursday, 17 March 2016. Douglas Coats of Marine Research Specialists (MRS) supervised scientific operations as Chief Scientist, and provided data-acquisition and navigational support during the survey. He also assisted with the deployment and recovery of the CTD and drifter, and collected meteorological measurements at each station. Crewmember William Skok managed deck operations and collected the Secchi depth measurements at each station.

Auxiliary Measurements

Auxiliary measurements and observations were collected during the vertical water-column profiling conducted at each of the six stations. Standard observations of weather and sea conditions, and beneficial uses, were augmented by visual inspection of the sea surface for floating particulates, oil sheens, and discoloration potentially related to the effluent discharge. Other auxiliary measurements collected at each station included wind speeds and air temperatures measured with a handheld Kestrel® 2000 Thermo-Anemometer, and oceanic flow measurements made throughout the survey area using a drogued drifter.

Additionally, at all six stations, a Secchi disk was lowered through the water column to determine its depth of disappearance. Secchi depths provide a visual measure of near-surface turbidity or water clarity. The depth of disappearance is inversely proportional to the average amount of organic and inorganic suspended material along a line of sight in the upper water column. As such, Secchi depths measure natural light penetration, which can be limited by increased suspended particulate loads from plankton blooms, onshore runoff, seafloor sediment resuspension, and wastewater discharge. They are also biologically meaningful because the depth of the euphotic zone, where most oceanic photosynthesis occurs, extends to approximately twice the Secchi depth.

Instrumental Measurements

A Sea Bird Electronics SBE-19plusV2 Seacat CTD instrument package collected measurements of conductivity, temperature, light transmittance, dissolved oxygen (DO), pH, and pressure during the March 2016 survey. The six seawater properties used to assess receiving-water quality in this report were derived from the continuously recorded output from the CTD's probes and sensors. Although pressure-housing limitations confine the CTD to depths less than 680 m (Table 3), this is well beyond the maximum depth of the deepest station in the outfall survey. The entire CTD was returned to the factory in January 2015 for full calibration and servicing. The transmissometer and DO probe were returned to the manufacturer in January 2016 for further servicing, repair, and calibration.

Table 3. CTD Specifications

Component	Units	Range	Accuracy	Resolution
Housing (19p-1a; Acetron Plastic)	m	0 to 680	—	—
Pump (SBE 5P)	—	—	—	—
Pressure (19p-2h; Strain-Gauge)	dBar	0 to 680	±1.7	± 0.10
Conductivity	Siemens/m	0 to 9	± 0.0005	± 0.00005
Salinity	‰	0 to 58	± 0.004	± 0.0004
Temperature	ºC	–5 to 35	± 0.005	± 0.0001
Transmissivity (WETLabs C-Star)[16]	%	0 to 100	± 0.3	± 0.03
Oxygen (SBE 43)	% Saturation	0 to 120	± 2	—
pH (SBE 18)	pH	0 to 14	± 0.1	—

The precision and accuracy of the various probes, as reported in manufacturer's specifications, are listed in Table 3. Salinity (‰) was calculated from conductivity measurements reported in units of Siemens/m. Density was derived from contemporaneous temperature (°C) and salinity data, and was expressed as 1000 times the specific gravity minus one, which is a unit of sigma-T (σ_t).

Assessments of all three of the physical parameters (salinity, temperature, and density) helped determine the lateral extent of the effluent plume during the towing phase of the survey. Additionally, during the vertical-profiling phase, they quantified layering, or vertical stratification and stability of the water column, which determines the behavior and dynamics of the effluent as it mixes with seawater within and beyond the ZID. Data on the three remaining seawater properties, light transmittance (water clarity), hydrogen-ion concentration (acidity/alkalinity – pH), and dissolved oxygen (DO), further characterized the receiving waters, and were used to assess compliance with water-quality criteria. Light transmittance was measured as a percentage of the initial intensity of a transmitted beam of light detected at the opposite end of a 0.25-m path. Transmissivity readings are reported relative to 100% transmission in air, so the maximum theoretical transmission in (pure) water is expected to be 91.3%.

Before beginning the mid-depth tow survey at 8:04 AM, the CTD was deployed beneath the sea surface for 11 minutes as the vessel was positioned to begin the first transect. Prior to deployment, the CTD package had been configured for horizontal towing with forward-looking probes. The protective cage around the CTD was fitted with a horizontal stabilizer wing and a depth-suppression weight was added to the towline to achieve near constant-depth tows.

Eight transects of mid-depth data were collected at an average depth near 8.2 m and an average speed of 1.60 m/s over the span of 34 minutes (Figure 6). Subsequently, at 8:43 AM, eight additional passes were made with the CTD at an average depth near 4.0 m. During this 31-minute shallow tow, vessel speed averaged 1.64 m/s. At the observed towing speeds and the 4 Hz sampling rate, at least 2.4 CTD measurements were collected for each meter traversed. This complies with the NPDES discharge permit requirement for minimum horizontal resolution of at least one sample per meter during at least five passes around and across the ZID at two separate depths, one within the surface mixed layer and one at mid-depth within the thermocline.

Contemporaneous navigation fixes recorded onboard the survey vessel were adjusted for CTD setback and aligned with time stamps on the internally recorded CTD data. The resulting data for the six seawater properties were then processed to produce horizontal maps within the upper and sub-thermocline portions of the water column.[17]

[16] 25-cm path length of red (650 nm) light
[17] Figures 8 and 9 later in this report

At 9:15AM, following completion of the last shallow transect, the CTD package was brought aboard the survey vessel and reconfigured for vertical profiling. The CTD was redeployed at 9:22AM, and was held beneath the surface for six minutes as the vessel was repositioned over Station RW6. The CTD was raised to within 0.5 m of the sea surface and profiling commenced. The CTD was lowered at a continuous rate of speed to the seafloor. Measurements at all six stations were collected during a single deployment of the CTD package by towing it below the water surface while transiting between adjacent stations.

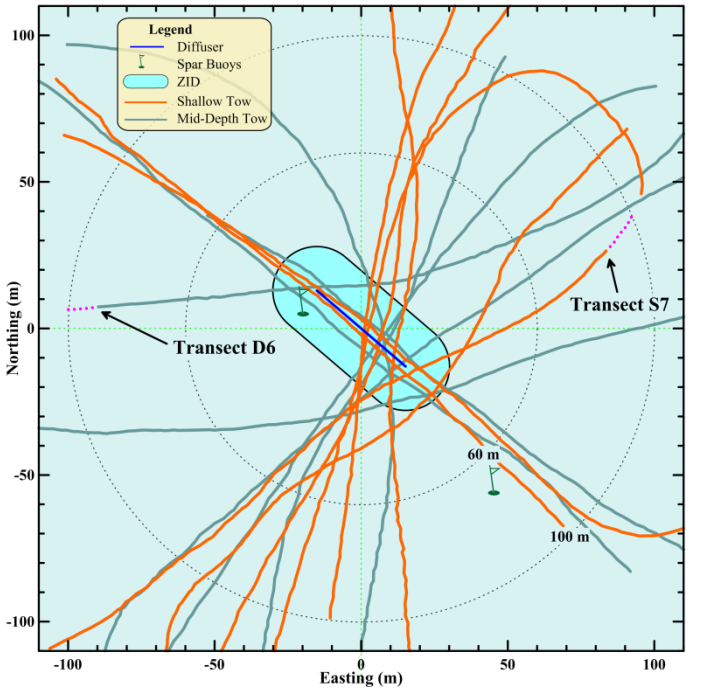

Figure 6. CTD Tracklines during the March 2016 Tow Surveys

Quality Control

During the vertical-profiling and horizontal-towing phases of the survey, real-time data were monitored for completeness and range acceptability. Although real-time monitoring indicated the recorded properties were complete and within acceptable coastal seawater ranges,[18] subsequent post-processing revealed several events that impacted portions of the data, resulting in the adjustment or exclusion of these data prior to initiating the compliance analysis. Specifically, review of the tow data revealed that the CTD changed depth when the vessel executed a turn at the beginning and end of each transect. The offsets in CTD depth are induced by changes in vessel speed and direction that are instituted to realign the vessel between each transect. Because of the complex interaction between turn radius, vessel speed, and CTD depth, the CTD's target depth cannot always be maintained at these times.

Because the discharge-related anomalies used in the compliance analysis are identified by comparing the amplitudes of measurements acquired at the same depth level, the ability to resolve anomalies with statistical certainty is compromised when data from different depth levels are combined in the horizontal maps. This is true whenever the water column is stratified, as was the case during the March 2016 survey.

However, the exclusion of portions of tow data did not adversely affect the compliance analysis. Only small portions of two transects exhibited depth offsets within the 100-m survey area (purple dotted lines in Figure 6). The remaining transects were long enough to fully encompass the 100-m survey area surrounding the diffuser structure. Specifically, the tow data that was included in the compliance analysis, shown by the solid orange and blue-green lines in Figure 6, met the permit monitoring requirement of at least five passes near the diffuser structure at each tow depth.

[18] Field sampling protocols employed during the survey generally followed the field operations manual for the Southern California Bight Study (SCBFMC 2002), which includes CTD cast-acceptability ranges listed in Table 2 of the manual.

RESULTS

The first-quarter receiving-water survey was conducted on the morning of Thursday, 17 March 2016. The receiving-water survey commenced at 7:42 AM with the deployment of the drogued drifter. Over the course of the ensuing 2.5 hours, offshore observations and measurements were collected as required by the NPDES monitoring program. The survey ended at 10:14 AM with the retrieval of the drogued drifter. Collection of required visual observations of the sea surface was generally unencumbered throughout the survey.

Auxiliary Observations

On the morning of 17 March 2016, skies were clear, with a sustained offshore breeze. Auxiliary observations were collected beginning at 9:57 AM, after completion of the vertical profiling phase of the survey. During the subsequent 15 minutes, each station was re-occupied beginning with Station RW1, and sequentially progressing toward the south. During that time, winds shifted from out of the east-northeast to the east-southeast. Average wind speeds, calculated over one-minute intervals, decreased from 6.2 kt to 4.6 kt (Table 4). Peak wind speeds fluctuated around a mean speed of 7.5 kt. A swell out of the northwest had a significant wave height of two-to-three feet. Air temperatures remained fairly constant and averaged 19.8°C, which was significantly higher than the 12.5°C sea surface temperature.

Table 4. Standard Meteorological and Oceanographic Observations

	Location[19]		Diffuser Distance	Time	Air	Cloud Cover	Wind Avg	Wind Max	Wind Dir (from)	Swell Ht/Dir	Secchi Depth
Station	Latitude	Longitude	(m)	(PDT)	(°C)	(%)	(kt)	(kt)	(°T)	(ft/°T)	(m)
RW1	35° 23.257' N	120° 52.509' W	94.2	9:57:01	19.9	0	6.2	8.5	60	2-3 NW	3.5
RW2	35° 23.231' N	120° 52.509' W	47.2	10:00:45	19.6	0	5.8	8.6	60	2-3 NW	3.5
RW3	35° 23.203' N	120° 52.504' W	5.8	10:03:28	19.0	0	5.7	6.2	60	2-3 NW	3.0
RW4	35° 23.179' N	120° 52.514' W	36.9	10:06:35	20.4	0	4.9	6.8	70	2-3 NW	3.0
RW5	35° 23.161' N	120° 52.506' W	59.0	10:09:35	20.2	0	5.2	8.4	100	2-3 NW	3.0
RW6	35° 23.136' N	120° 52.513' W	106.4	10:12:08	19.7	0	4.6	6.5	100	2-3 NW	3.0

Although there was no evidence of floating particulates, oil sheens, or any discoloration of the sea surface associated with wastewater constituents, biofilm particulates suspended within the upper water column were visually apparent during portions of the March 2016. Biofilm particulates are not present in wastewater prior to discharge at the treatment plant, but line the interior surface of the outfall pipe. At the higher effluent discharge rates during mid-morning hours, small pieces of biofilm occasionally detach from the outfall pipe and mix with the wastewater discharged offshore. These distinctive black and white particulates have been observed during some of the past water-quality surveys. They are, however, unrelated to the particulate loading within MBCSD effluent, and have little bearing on the transmittance of natural light.

In addition, the signature of the effluent plume was visually apparent northeast of the ZID during portions of the survey. An area of reduced capillary waves on the sea surface was observed at various times during the March 2016 survey. This surface expression of the plume has been seen occasionally during past surveys that were conducted when the seastate was relatively calm. The surface-boil feature is a physical manifestation of the surfacing effluent plume and is a clear indication that the plume had risen to the

[19] Locations are the vessel positions at the time the Secchi depths were measured. These depart from the CTD profile locations listed in Table 2 because they were collected after completion of the CTD profiling.

surface rather than being trapped at depth. Again, the presence of this feature has no significant aesthetic impact on the sea surface, or on the transmittance of natural light through the water column.

An area of increased subsurface turbidity was also seen in conjunction with the plume during the tow surveys. However, the presence of wastewater particulates did not contribute significantly to the observed turbidity. On the day of the survey, the 22 mg/L suspended-solid concentration measured onshore within effluent prior to discharge was too small to cause the observed decrease in transmissivity in the upper water column. Instead, as in past surveys where shallow turbidity signatures were observed, turbid ambient seawater near the seafloor had been entrained into the plume shortly after discharge, and was subsequently carried upward by the buoyant plume.

Naturally occurring resuspension processes can cause marked increases in turbidly immediately above the seafloor. During upwelling, the shoreward transport of offshore waters along the seafloor occasionally generates increased turbulence and shear within a benthic nepheloid layer (BNL). These thin, transient, particle-rich layers form when lightweight flocs of detritus are resuspended by the turbulence generated from bottom currents. These layers are a widespread phenomenon on continental shelves (Kuehl et al. 1996) and have been regularly documented in past surveys conducted within Estero Bay.

However, the subsurface turbidity plume was not visually or instrumentally apparent during the vertical-profiling and auxiliary-observation phases of the survey. This suggests that the transient BNL had either dissipated or moved out of the survey area by that time, and was not contributing significant particulate loads during initial mixing near the seafloor. Notably, flow direction, as measured by the drogued drifter (Figure 3), changed shortly before vertical profiling began at 9:27 AM, suggesting that the flow regime responsible for BNL formation was no longer present within the survey area.

Secchi depths measured during the auxiliary-observation phase of the survey (Table 4), did not exhibit a marked reduction at northern Stations (RW1, RW2, and RW3) that would be indicative of a reduction in the transmission of ambient light due to the presence of the turbidity plume. Ranging between 3.0 m and 3.5 m, the Secchi depths demonstrated that a relatively shallow, 6 m to 7 m euphotic zone was uniformly present at the time of the survey. The restricted light penetration resulted from upwelling-induced increases in plankton density within the upper water column. During upwelling, nutrients carried upward into the euphotic zone are assimilated by phytoplankton, whose populations increase and, along with their associated zooplanktonic predators; their elevated densities reduce the transmittance of ambient light.

Communication with plant personnel and subsequent review of effluent discharge properties on the day of the survey, confirmed that the treatment process was performing well at time of the survey. The 0.892 million gallons of effluent discharged on 17 March had a temperature of 19°C, a suspended-solids concentration of 22 mg/L, and a pH of 7.6. A marginally quantifiable amount of oil and grease (5.2 mg/L) was present in the effluent sample collected a few days prior to the survey. The biochemical oxygen demand (BOD) of the effluent measured two days prior to the survey, on 15 March, was 52 mg/L.

Instrumental Observations

Data collected during vertical profiling were processed in accordance with standard procedures (SCCWRP 2002), and are collated within 0.5-m depth intervals in Table 5. Data collected during the March 2016 survey reflect moderately stratified conditions within Estero Bay indicative of the onset of a major upwelling event that marked the beginning of the spring transition (refer to the inset in Figure 5).

Table 5. Vertical Profile Data Collected on 17 March 2016

Depth (m)	Temperature (°C)						Salinity (‰)					
	RW-1	RW-2	RW-3	RW-4	RW-5	RW-6	RW-1	RW-2	RW-3	RW-4	RW-5	RW-6
0.5	12.539	12.509	12.519	12.518	12.515	12.531	33.453	33.458	33.452	33.447	33.452	33.452
1.0	12.545	12.527	12.516	12.512	12.515	12.534	33.456	33.450	33.450	33.448	33.452	33.451
1.5	12.533	12.501	12.486	12.440	12.491	12.530	33.455	33.448	33.448	33.445	33.451	33.451
2.0	12.452	12.405	12.429	12.355	12.469	12.499	33.449	33.440	33.444	33.442	33.452	33.453
2.5	12.371	12.307	12.277	12.330	12.435	12.455	33.447	33.435	33.426	33.443	33.454	33.456
3.0	12.257	12.245	12.259	12.255	12.401	12.404	33.441	33.433	33.430	33.449	33.462	33.463
3.5	12.202	12.167	12.312	12.264	12.358	12.345	33.455	33.430	33.437	33.474	33.470	33.473
4.0	12.234	12.146	12.212	12.269	12.328	12.309	33.477	33.436	33.428	33.479	33.475	33.478
4.5	12.237	12.133	12.097	12.267	12.314	12.289	33.479	33.442	33.427	33.479	33.478	33.480
5.0	12.225	12.148	12.072	12.271	12.302	12.253	33.480	33.459	33.432	33.481	33.480	33.482
5.5	12.199	12.160	12.024	12.276	12.290	12.220	33.476	33.473	33.429	33.482	33.481	33.486
6.0	12.187	12.152	12.039	12.274	12.243	12.191	33.475	33.474	33.433	33.483	33.485	33.489
6.5	12.161	12.141	12.096	12.267	12.174	12.163	33.469	33.475	33.447	33.484	33.486	33.491
7.0	12.129	12.135	12.117	12.255	12.145	12.144	33.471	33.480	33.457	33.485	33.491	33.492
7.5	12.089	12.117	12.095	12.194	12.106	12.083	33.482	33.484	33.464	33.488	33.495	33.496
8.0	12.063	12.104	12.085	12.140	12.042	12.011	33.491	33.491	33.475	33.492	33.499	33.503
8.5	12.036	12.099	12.086	12.093	12.027	11.964	33.498	33.498	33.487	33.496	33.503	33.510
9.0	12.026	12.041	12.078	12.077	12.010	11.919	33.500	33.504	33.490	33.499	33.505	33.514
9.5	11.931	12.001	12.008	12.032	11.982	11.898	33.506	33.509	33.505	33.503	33.509	33.518
10.0	11.879	11.925	11.954	11.967	11.927	11.891	33.514	33.515	33.512	33.510	33.514	33.520
10.5	11.826	11.859	11.923	11.893	11.893	11.888	33.519	33.522	33.517	33.518	33.519	33.521
11.0	11.824	11.846	11.850	11.855	11.883	11.874	33.522	33.524	33.523	33.524	33.522	33.523
11.5	11.829	11.839	11.847	11.835	11.876	11.848	33.524	33.526	33.525	33.527	33.523	33.525
12.0	11.831	11.834	11.846	11.824	11.868	11.835	33.525	33.527	33.526	33.528	33.525	33.527
12.5	11.822	11.831	11.840	11.824	11.833	11.823	33.526	33.528	33.528	33.529	33.527	33.528
13.0	11.817	11.830	11.836	11.819	11.812	11.819	33.527	33.529	33.528	33.530	33.529	33.528
13.5	11.811	11.828	11.834	11.809	11.812	11.817	33.528	33.530	33.529	33.531	33.530	33.528
14.0	11.804	11.822	11.838	11.806	11.811	11.817	33.529	33.531	33.472	33.531	33.530	33.529
14.5	11.801	11.819	11.833	11.806	11.811	11.819	33.530	33.532	33.463	33.532	33.530	33.529
15.0	11.800	11.821	11.814	11.807	11.812	11.819	33.530	33.532	33.514	33.532	33.530	33.529
15.5	11.811	11.822	11.807	11.809	11.812	11.820	33.530	33.532	33.532	33.532	33.530	33.529
16.0	11.823	11.824	11.802	11.813	11.815	11.821	33.529	33.532	33.533	33.532	33.530	33.529
16.5			11.803	11.814	11.815	11.823			33.533	33.531	33.531	33.528
17.0						11.826						33.527

Table 5. Vertical Profile Data Collected on 17 March 2016 (continued)

Depth (m)	Density (σ_t)						pH					
	RW-1	RW-2	RW-3	RW-4	RW-5	RW-6	RW-1	RW-2	RW-3	RW-4	RW-5	RW-6
0.5	25.284	25.285	25.287	25.286	25.289	25.284	7.944	7.941	7.941	7.942	7.941	7.942
1.0	25.286	25.285	25.287	25.286	25.289	25.284	7.948	7.944	7.942	7.942	7.942	7.943
1.5	25.287	25.288	25.291	25.297	25.293	25.285	7.949	7.945	7.942	7.942	7.941	7.942
2.0	25.299	25.301	25.299	25.312	25.298	25.292	7.946	7.941	7.941	7.938	7.942	7.942
2.5	25.312	25.315	25.315	25.317	25.306	25.304	7.941	7.935	7.938	7.935	7.940	7.941
3.0	25.330	25.326	25.321	25.336	25.319	25.319	7.936	7.930	7.930	7.932	7.939	7.940
3.5	25.351	25.339	25.316	25.354	25.333	25.338	7.928	7.925	7.928	7.930	7.938	7.938
4.0	25.362	25.347	25.328	25.357	25.343	25.349	7.928	7.922	7.929	7.931	7.936	7.935
4.5	25.363	25.354	25.350	25.358	25.348	25.354	7.929	7.919	7.925	7.929	7.933	7.933
5.0	25.366	25.364	25.358	25.358	25.351	25.363	7.929	7.919	7.919	7.929	7.933	7.931
5.5	25.368	25.373	25.365	25.358	25.355	25.371	7.927	7.921	7.916	7.929	7.932	7.930
6.0	25.369	25.375	25.365	25.359	25.367	25.380	7.927	7.922	7.911	7.930	7.932	7.927
6.5	25.370	25.378	25.365	25.361	25.380	25.386	7.926	7.921	7.912	7.930	7.928	7.925
7.0	25.377	25.383	25.369	25.364	25.390	25.391	7.925	7.921	7.914	7.930	7.927	7.924
7.5	25.393	25.389	25.378	25.378	25.400	25.406	7.924	7.922	7.914	7.928	7.924	7.921
8.0	25.405	25.397	25.389	25.391	25.416	25.424	7.921	7.920	7.915	7.925	7.921	7.919
8.5	25.415	25.404	25.398	25.403	25.421	25.438	7.920	7.920	7.916	7.923	7.919	7.915
9.0	25.419	25.420	25.402	25.409	25.426	25.451	7.919	7.918	7.916	7.921	7.915	7.910
9.5	25.442	25.431	25.426	25.420	25.435	25.457	7.918	7.916	7.915	7.918	7.915	7.906
10.0	25.458	25.450	25.443	25.438	25.449	25.460	7.917	7.912	7.914	7.915	7.910	7.905
10.5	25.472	25.467	25.452	25.458	25.459	25.462	7.913	7.906	7.909	7.910	7.906	7.903
11.0	25.474	25.472	25.471	25.470	25.463	25.465	7.911	7.902	7.905	7.904	7.904	7.902
11.5	25.475	25.474	25.473	25.476	25.466	25.472	7.907	7.901	7.903	7.902	7.902	7.901
12.0	25.475	25.476	25.474	25.479	25.468	25.476	7.907	7.900	7.902	7.900	7.901	7.899
12.5	25.477	25.478	25.476	25.480	25.477	25.479	7.905	7.900	7.901	7.899	7.900	7.898
13.0	25.480	25.479	25.477	25.482	25.482	25.480	7.905	7.900	7.900	7.898	7.898	7.897
13.5	25.482	25.480	25.477	25.484	25.483	25.481	7.903	7.899	7.899	7.898	7.897	7.897
14.0	25.484	25.482	25.433	25.485	25.483	25.481	7.902	7.899	7.899	7.897	7.896	7.896
14.5	25.485	25.483	25.427	25.485	25.483	25.480	7.901	7.897	7.896	7.897	7.896	7.896
15.0	25.485	25.482	25.470	25.485	25.483	25.480	7.901	7.898	7.895	7.896	7.895	7.897
15.5	25.483	25.482	25.485	25.485	25.483	25.480	7.902	7.897	7.895	7.897	7.895	7.896
16.0	25.480	25.482	25.487	25.484	25.483	25.480	7.900	7.897	7.895	7.896	7.895	7.897
16.5			25.487	25.483	25.483	25.479			7.895	7.896	7.895	7.896
17.0						25.478						7.898

Table 5. Vertical Profile Data Collected on 17 March 2016 (continued)

Depth (m)	Dissolved Oxygen (mg/L)						Transmissivity (%)					
	RW-1	RW-2	RW-3	RW-4	RW-5	RW-6	RW-1	RW-2	RW-3	RW-4	RW-5	RW-6
0.5	6.882	6.745	6.840	6.843	6.850	6.863	75.893	75.949	76.308	76.485	76.716	77.562
1.0	6.857	6.802	6.771	6.762	6.831	6.874	76.179	76.493	76.392	76.516	76.814	77.503
1.5	6.751	6.626	6.631	6.589	6.792	6.818	76.366	76.908	76.458	76.357	76.807	77.610
2.0	6.642	6.482	6.383	6.544	6.772	6.781	76.382	76.047	76.549	75.980	76.297	77.407
2.5	6.433	6.338	6.441	6.587	6.768	6.814	75.584	74.950	76.508	75.967	76.020	77.214
3.0	6.424	6.247	6.515	6.799	6.778	6.857	74.189	75.444	76.453	75.751	75.161	76.391
3.5	6.513	6.240	6.271	6.809	6.838	6.807	71.628	76.379	76.768	73.401	73.780	73.381
4.0	6.515	6.269	6.128	6.817	6.857	6.696	68.670	76.527	76.557	67.689	71.558	70.338
4.5	6.497	6.378	6.107	6.827	6.809	6.578	67.595	74.823	75.964	66.505	69.776	72.034
5.0	6.480	6.436	6.029	6.842	6.788	6.763	67.092	73.991	75.888	65.785	69.512	75.499
5.5	6.472	6.389	6.135	6.767	6.435	6.714	66.907	71.854	75.241	65.565	69.853	77.592
6.0	6.424	6.364	6.229	6.713	6.108	6.397	66.199	71.671	75.639	65.670	69.357	73.976
6.5	6.311	6.316	6.249	6.534	6.108	6.193	65.867	73.167	75.748	65.971	74.596	74.144
7.0	6.201	6.249	6.177	6.169	6.028	6.008	65.806	73.172	75.468	67.863	83.576	82.247
7.5	6.136	6.192	6.140	6.073	5.935	5.906	67.990	73.088	74.598	71.516	86.568	86.810
8.0	6.106	6.167	6.144	6.014	5.943	5.843	70.629	75.010	77.610	79.467	87.089	87.869
8.5	6.066	6.019	6.124	6.001	5.906	5.807	73.229	76.793	78.955	84.140	87.652	87.690
9.0	5.816	5.964	5.936	5.927	5.866	5.789	73.491	77.571	79.241	84.694	87.601	86.395
9.5	5.764	5.856	5.903	5.885	5.813	5.763	76.000	79.474	79.449	86.208	87.346	85.921
10.0	5.723	5.830	5.863	5.801	5.802	5.773	81.999	80.033	79.801	85.778	86.331	85.927
10.5	5.746	5.793	5.773	5.756	5.779	5.738	90.246	75.532	79.256	84.699	84.885	86.026
11.0	5.763	5.769	5.777	5.707	5.769	5.680	89.979	69.812	74.055	80.866	83.337	85.469
11.5	5.765	5.725	5.760	5.691	5.738	5.689	86.274	66.694	72.141	77.075	82.554	85.854
12.0	5.731	5.730	5.730	5.687	5.669	5.681	81.987	67.800	72.380	77.322	82.228	86.531
12.5	5.730	5.718	5.725	5.669	5.644	5.665	81.089	69.150	69.981	78.024	83.591	86.404
13.0	5.722	5.711	5.718	5.641	5.655	5.666	79.721	69.249	70.358	78.266	84.994	86.173
13.5	5.675	5.664	5.682	5.643	5.652	5.665	76.703	69.527	71.299	78.885	85.172	85.634
14.0	5.675	5.651	5.655	5.641	5.657	5.668	76.849	67.979	70.968	80.320	85.428	84.787
14.5	5.660	5.655	5.651	5.644	5.647	5.664	81.253	65.772	71.739	80.469	84.867	84.106
15.0	5.675	5.636	5.635	5.634	5.638	5.668	80.337	64.375	73.773	80.809	84.377	83.969
15.5	5.684	5.634	5.612	5.640	5.640	5.660	73.526	63.959	73.830	80.108	83.339	83.960
16.0	5.674	5.633	5.619	5.631	5.645	5.661	65.282	61.361	74.777	79.424	81.011	82.963
16.5			5.609	5.640	5.642	5.658			72.506	76.366	80.684	81.645
17.0						5.665						80.395

Upwelling of varying intensity occurs most of the year along the central California coast, with the strongest upwelling winds beginning in March or April and extending through the summer. The intensity of upwelling tends to decline into fall, although pulses of sustained northwesterly winds still occur. An intense upwelling event results in the rapid influx of dense, cold, saline water at depth and leads to a sharp thermocline, halocline, and pycnocline where temperature, salinity, and density change rapidly over a small vertical distance. Under these highly stratified conditions, isotherms crowd together to form a density interface that inhibits the vertical exchange of nutrients and other water properties, traps the effluent plume at depth, and reduces the initial dilution of the effluent plume.

If the upwelling winds are only of moderate strength, occur only briefly, or have not occurred recently; the contrast between the surface and deep watermasses is reduced, and stratification appears as a more gradual vertical change in seawater properties below the surface mixed layer. This was the case during the March 2016 survey where the upwelling signatures in the vertical profiles unaffected by the discharge appear as a steady change with depth (between 2 m and 10 m in Figure 7ef). Absent are sharply defined interfaces where large changes in seawater properties occur over a limited vertical extent, signatures that are normally indicative of strong, recent upwelling conditions. In contrast, the thermocline that was present during the March 2016 survey extended across half of the water column.

This gradual transition zone separated a relatively uniform mixed layer, which extended down to 2 m, from a 7-m-thick seawater mass situated immediately above the sea floor. Within this weak thermocline, seawater properties exhibited steadily increasing or decreasing values that were determined by well-defined oceanographic processes. In particular, temperature (red lines), pH (olive-colored lines), and to some extent DO (dark blue lines) steadily decrease with increasing depth between 2 and 10 m. These decreases are mirrored by a halocline and pycnocline, where salinity (green lines) and density (black lines) steadily increase with depth.

These gradual vertical changes represent the transition zone between the surface mixed layer and the deep offshore watermass that migrated shoreward along the seafloor as part of the upwelling process. The seawater properties of this deep watermass originate within the northward-flowing Davidson undercurrent that carries warmer, more saline, and less oxygenated waters out of the Southern California Bight and northward along the central California coast. Because of their origin, ambient seawater properties measured at depth during the March 2016 survey differed from that of ambient seawater within the upper water column of Estero Bay. Specifically, the seawater was colder, saltier, and nutrient-rich but oxygen-poor. Because the seawater had not been in recent direct contact with the atmosphere, biotic respiration and decomposition had depleted its DO levels (dark blue lines below 7 m in Figure 7ef). Additionally, at depth, biotic respiration and decomposition produced carbon dioxide (CO_2), and in its dissolved state, the increased concentration of carbonic acid appears as a concomitant decline in pH (olive-colored lines).

Meanwhile, within the surface mixed layer, nutrient-rich seawater brought to the sea surface by the recent upwelling facilitated phytoplankton blooms that produced oxygen, consumed carbon dioxide (CO_2), and decreased water clarity (light blue lines). The increased presence of plankton at the top of transition zone (thermocline) near 5 m caused a 14% decrease in transmissivity compared to that of the deeper water mass (light blue lines in Figure 7ef). As mentioned previously, a sharp decline in transmissivity within a thin BNL immediately above the seafloor was conspicuously absent in the vertical profiles.

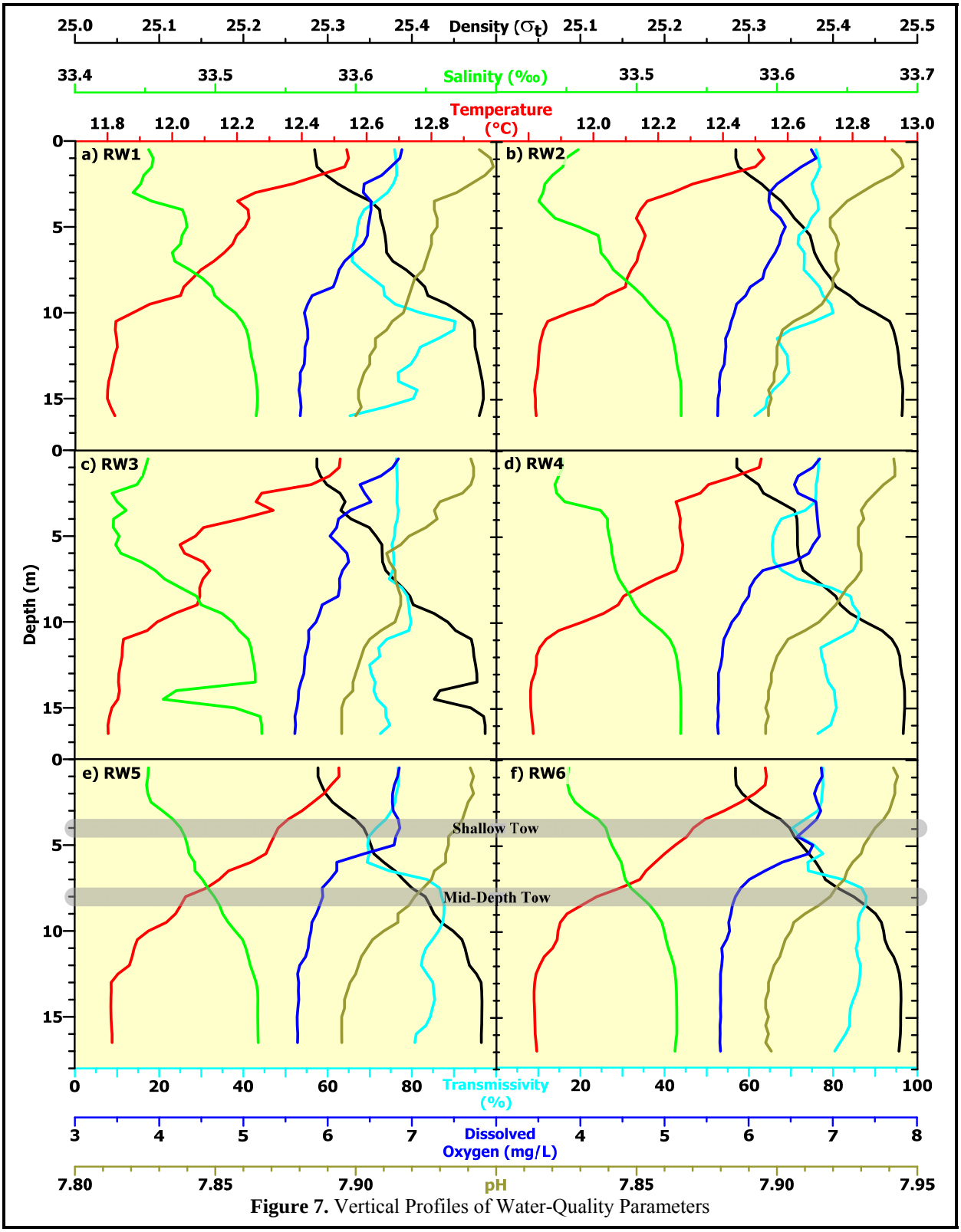

Figure 7. Vertical Profiles of Water-Quality Parameters

The degree of vertical stratification within the receiving seawater is important for understanding the dynamics of effluent dispersion at the time of the survey. For example, when the water column is strongly stratified by upwelling, the rising plume can become trapped at depth within the water column, thereby limiting its full capacity for dilution. However, this was not the case during the March 2016 survey. At that time, the water column was only moderately stratified, and as mentioned before, visual manifestations of the discharge plume were observed near the sea surface northeast of the diffuser structure. Accordingly, the signature of the effluent plume was captured at or near the sea surface in the profile data collected at the remaining stations (Figure 7abcd). It appears as excursions in water properties that depart from the more-regular vertical structure seen in Figure 7ef.

The vertical profiles measured at Station RW3 (Figure 7c) are particularly interesting because the plume was encountered twice, at two different stages in the dilution process. The CTD began the downcast at a location northeast of the ZID boundary, and transited most of the ZID toward the southwest as it was lowered to the seafloor (see the upper right inset in Figure 2). At the beginning of the cast, it captured the plume signature near the sea surface, as documented by the reduced salinity between 2 m and 6 m (green line in Figure 7c). At that point, the initial dilution process was nearly complete.

As the CTD approached the seafloor, it again encountered the plume at a depth near 14.5 m when it passed directly over the diffuser structure and captured mixing conditions shortly after discharge. The plume's low salinity relative to ambient salinity at that depth is readily apparent (sharp drop in salinity shown by the green line between 13.5 m and 15.5 m in Figure 7c). The plume was also very buoyant at that location, as indicated by the sharp reduction in density that coincides with the depth of the salinity anomaly (black line in Figure 7c). At that early stage in the dilution process, the plume was continuing to ascend and mix within the water column. Nevertheless, the effluent's signature in other water properties, including transmissivity (light blue line) had largely dissipated, as indicated by the absence of sharp changes that correspond to the salinity and density anomalies.

The tow surveys also captured the signature of the plume in an area northeast of the diffuser structure (Figures 8 and 9). The mid-depth tow delineated the weak signature of the plume in the middle of the thermocline at a depth of 8.2 m (Figure 8). There, the plume was of limited lateral extent, and largely confined to the ZID. The strongest mid-depth plume signature was observed almost directly above the open section of the diffuser structure and was highly localized within the ZID (delineated in red along the southeast section of the diffuser structure in Figure 8b). This salinity anomaly coincides with marked reductions in density (Figure 8c) that indicate the plume was highly buoyant at that point, and would continue to mix rapidly during its ascent through the rest of the water column. Thus, the mid-depth tow captured the early stages of the initial dilution process.

Although smaller in amplitude, another pool of reduced salinity was measured by the mid-depth tow along the northern boundary of the ZID (delineated in dark blue and green in Figure 8b). However, this portion of the plume was not buoyant because there was no corresponding density decrease at that location (Figure 8c), largely because a potential decrease in density due to the reduced salinity was offset by slightly lower temperatures (delineated in dark blue and green along the northern ZID boundary in Figure 8a). The reduced temperature at that location arose because the plume entrained cooler ambient seawater at depth. It could not have been caused by the influence of dilute wastewater because effluent was much warmer (19°C) than the receiving seawater (11.8°C).

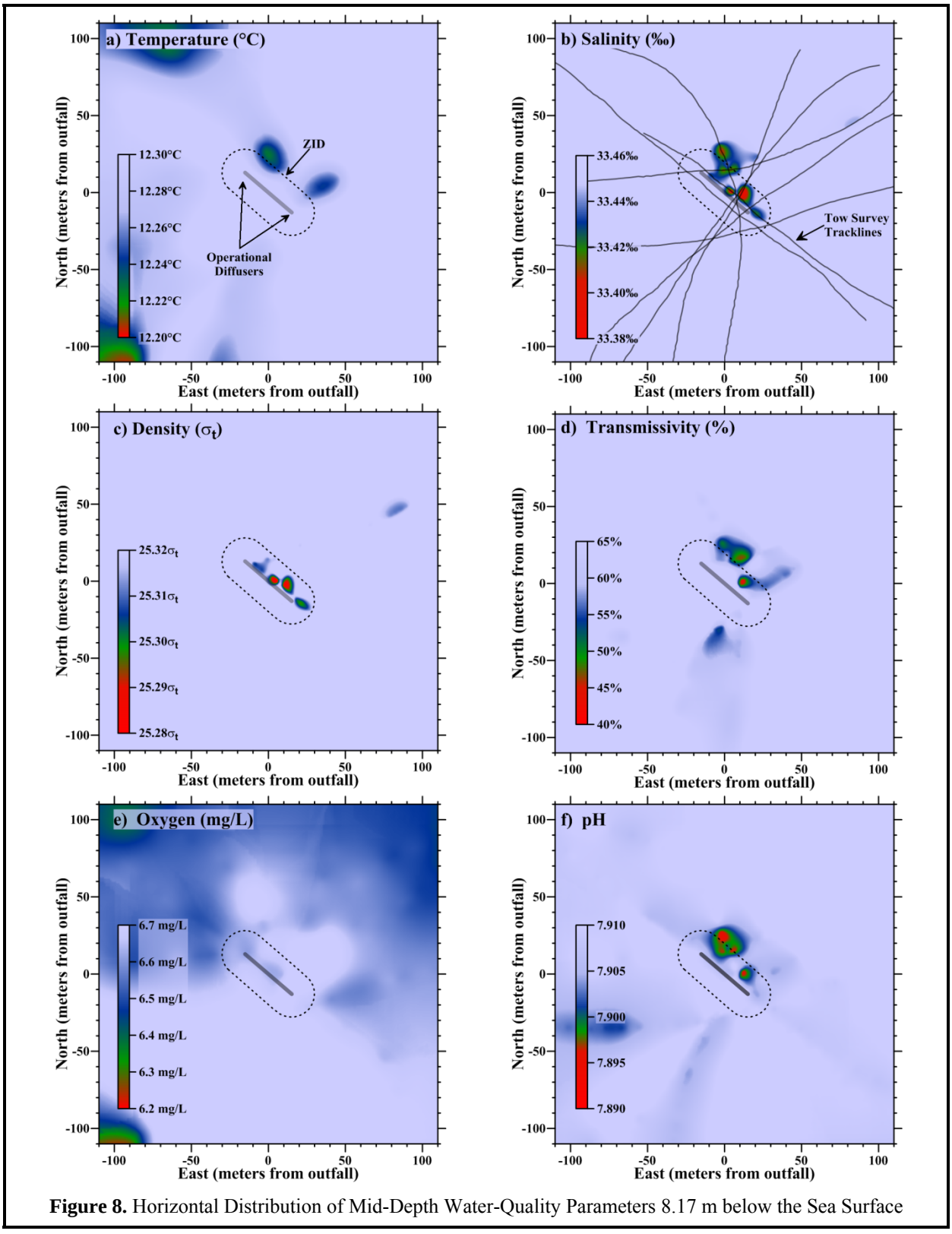

Figure 8. Horizontal Distribution of Mid-Depth Water-Quality Parameters 8.17 m below the Sea Surface

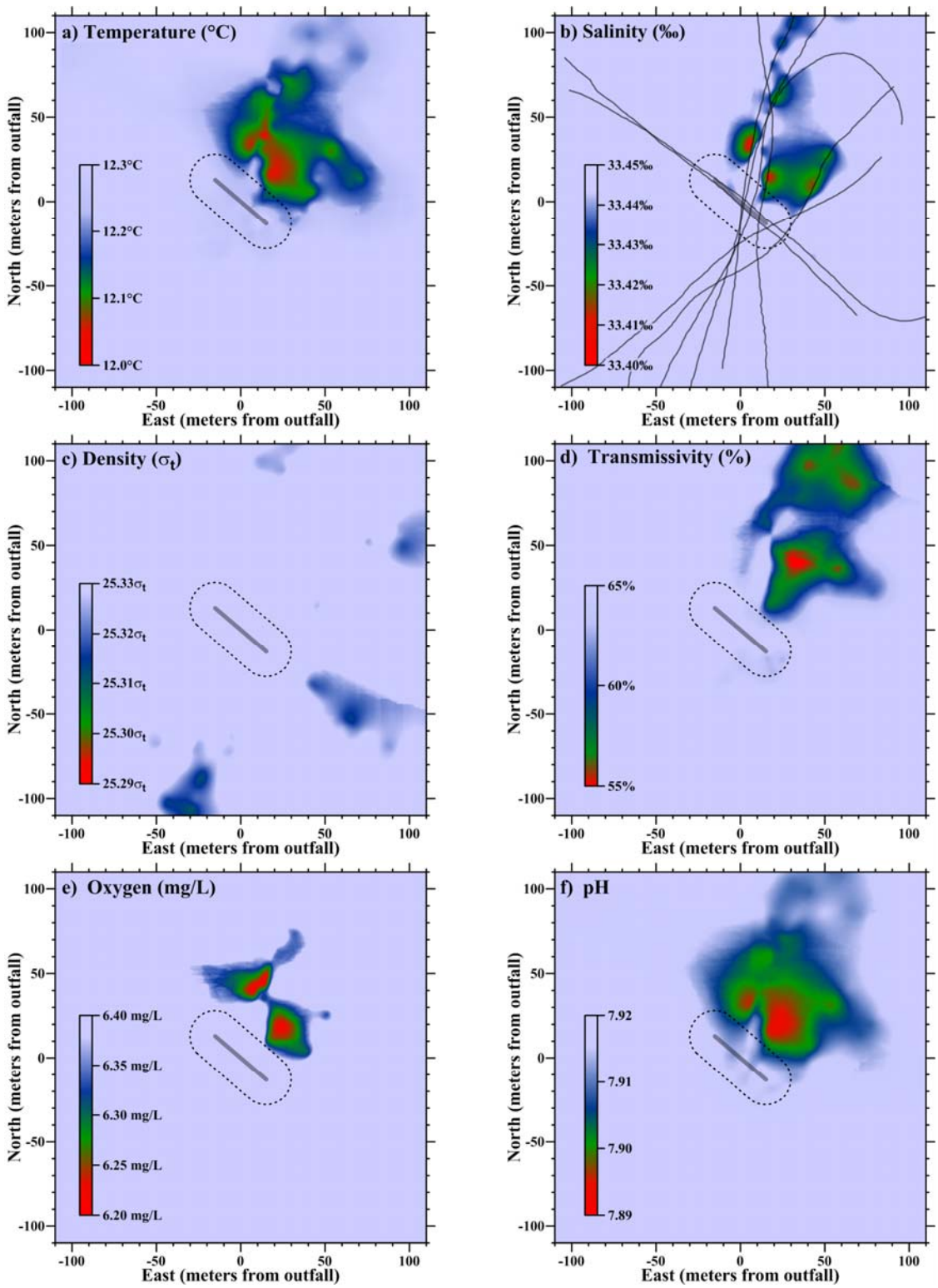

Figure 9. Horizontal Distribution of Shallow Water-Quality Parameters 3.96 m below the Sea Surface

It is important to distinguish plume signatures that are caused by the presence of effluent constituents, exemplified by sharp reductions in salinity and density, from those caused by the upward transport of ambient seawater entrained near the seafloor shortly after discharge. Close to the seafloor, intense mixing is driven by the momentum of the effluent's ejection from the individual diffuser ports. Subsequent turbulent mixing caused by the plume's ascent through the water column is less intense, and as a result, the dilute effluent plume tends to retain the ambient seawater properties it acquired at the seafloor. These deep seawater properties can become apparent as a signature of the buoyant effluent plume when they are juxtaposed against the ambient seawater characteristics in the mid and upper water column. These entrainment-generated anomalies are only apparent, however, when the water column is sufficiently stratified to cause a perceptible contrast between the shallow and deep ambient seawater properties.

Because of moderate stratification at the time of the March 2016 survey, mid-depth entrainment-generated anomalies were apparent in most water properties except for DO at mid-depth (Figures 8adf versus Figure 8e). In addition to the reduced temperature at mid-depth along the northern ZID boundary (Figure 8a), both transmissivity (Figure 8d) and pH (Figure 8f) exhibited reductions at the same locations as the salinity anomalies in Figure 8b. In contrast, the DO field was relatively uniform at mid depth (Figure 8e). The mid-depth plume did not exhibit a perceptible DO signature because the seawater entrained at depth had a DO concentration that was close to that of the ambient seawater at 8 m (dark blue lines in Figure 7ef). The vertical profiles of temperature (red lines) and pH (olive lines), on the other hand, exhibited a distinct decrease with increasing depth below 8 m. The upward transport of seawater with this reduced temperature and pH accounted for the minima seen during the mid-depth tow (Figure 8af).

However, the transmissivity reduction observed within the plume during the mid-depth tow (Figure 8d) cannot be as easily explained by the vertical gradients seen in the profile data. The transmissivity profiles (light blue lines in Figure 7ef) were relatively uniform within the lower water column during the vertical profiling phase of the survey, which occurred 1 hr 20 min after the mid-depth tow. The slight 6% variation with depth was far too small to account for the 20% transmissivity decrease seen within the plume during the mid-depth tow (Figure 8d). Instead, as described previously, the mid-depth transmissivity anomaly resulted from entrainment of turbid seawater within a transient BNL that was present during the towing phase of the survey, but absent during the subsequent vertical-profiling phase.

The legacies of entrainment anomalies can be particularly long-lived, remaining apparent within the water column well after completion of the initial dilution process. As such, these anomalies provide useful tracers of the diffuse effluent plume during and after the completion of the initial dilution process. However, such anomalies are irrelevant to the receiving-water compliance assessment because the permit restricts attention to water-quality changes caused solely by the presence of wastewater constituents rather than by a simple relocation of ambient seawater.

Because of their longevity and greater contrast with surrounding seawater, entrainment anomalies measured during the shallow tow were generally larger in amplitude and spatial extent (Figure 9adef). At the 4-m shallow tow depth, ambient seawater was much higher in temperature, DO, and pH than at mid-depth (red, dark blue, and olive lines in Figure 7ef), and thus provided a greater contrast with the deep seawater properties entrained within the plume. Although the plume's salinity signature extended over a much wider area (compare Figure 9b with Figure 8b), its amplitude was smaller, indicating a higher level of dilution had been achieved. The absence of a concomitant density anomaly (Figure 9c) indicates that the plume had achieved neutral buoyancy as it approached the sea surface and spread laterally. This change in plume dynamics marked the end of the initial dilution process.

Outfall Performance

The efficacy of the outfall can be evaluated through a comparison of dilution levels measured at the time of the March 2016 survey, and dilutions anticipated from modeling studies that were codified in the discharge permit through limits imposed on effluent constituents. Specifically, the critical initial dilution applicable to the MBCSD outfall was conservatively estimated to be 133:1 (Tetra Tech 1992). That is, dispersion modeling estimated that, at the conclusion of the minimum expected initial mixing, 133 parts of ambient seawater would have mixed with each part of wastewater.

The 133:1 dilution estimate was based on worst-case modeling under highly stratified conditions, where trapping of the plume below a strong thermocline would curtail the additional buoyant mixing normally experienced during the plume's ascent through the entire water column. Additionally, the modeling assumed quiescent oceanic flow conditions, thereby restricting initial mixing processes to the ZID. Under those conditions, the modeling predicted that a 133:1 dilution would be achieved after the plume rose only 9 m from the seafloor, whereupon it would become trapped, ceasing to ascend further in the water column. At that point, the plume would spread laterally with dilution occurring at a much-reduced rate. A 9-m ascent at the MBCSD outfall translates into a trapping depth that is 6.4 m below the sea surface. As described below, however, the dilution levels observed during the March 2016 survey were much higher than the 133:1 predicted by the modeling, and were measured at depths greater than the trapping depth predicted by the modeling.

The conservative nature of the critical initial dilution determined from the modeling is an important consideration because it was used to specify permit limitations on chemical concentrations in wastewater discharged from the treatment plant. These end-of-pipe effluent limitations were back calculated from the receiving-water objectives in the COP (SWRCB 2005) using the projected 133-fold dilution determined from the modeling. Application of a higher critical dilution would relax the stringent end-of-pipe effluent limitations thought necessary to meet COP objectives after initial dilution is complete.

End-of-pipe limitations on contaminant concentrations within discharged wastewater were based on the definition of dilution (Fischer et al. 1979). From the mass-balance of a conservative tracer, the concentration of a particular chemical constituent within effluent before discharge (C_e) can be determined from Equation 1.

$$C_e \equiv C_o + D(C_o - C_s) \qquad \text{Equation 1}$$

where: C_e = the concentration of a constituent in the effluent,
C_o = the concentration of the constituent in the ocean after dilution by D (i.e., the COP receiving-water objective),
D = the dilution expressed as the volumetric ratio of seawater mixed with effluent, and
C_s = the background concentration of the constituent in ambient seawater.

By rearranging Equation 1, the actual dilution achieved by the outfall can be determined from measured seawater anomalies. This measured dilution can then be compared with the critical dilution factor determined from modeling. Salinity is an especially useful tracer because it directly reflects the magnitude of ongoing dilution. The regions of slightly lower salinity apparent northeast of the diffuser structure in both of the tow-survey maps (Figures 8b and 9b) were induced by the presence of dilute wastewater. These salinity anomalies document mixing processes within the effluent plume shortly after discharge, and as it subsequently rose through the water column and approached the sea surface.

The amplitudes of these salinity anomalies quantify the magnitude of wastewater dilution at the various stages of the initial mixing process. By rearranging Equation 1, the dilution ratio (D) can be computed from the salinity anomaly ($A = C_o - C_s$) as:

$$D \equiv \frac{(C_e - C_o)}{(C_o - C_s)} \propto -A^{-1} \qquad \text{Equation 2}$$

The salinity concentration within MBCSD effluent (C_e)[20] is generally small compared to that of the receiving seawater and, after dilution by more than 133-fold, the salinity of the effluent-seawater mixture is close to ambient salinity. Consequently, to a close approximation, dilution levels are inversely proportional to the amplitude of the salinity anomaly. Thus, a lower effluent dilution at a given location within the receiving waters is directly mirrored by a larger salinity reduction.

The lowest salinities (<33.38‰) measured during the March 2016 survey were recorded 3.5 m from the diffuser structure during the second transect of the mid-depth tow survey (red shading in Figure 8b). The lowest of these measured salinities corresponded to a reduction of 0.135‰ below the mean ambient salinity (33.478‰) measured at the tow depth, but well beyond the influence of the discharge.

From Equation 2, that salinity anomaly corresponds to a dilution of 240-fold (Figure 10), which is well above the 133:1 critical initial dilution used to establish limits on contaminant concentrations in wastewater. In addition, this dilution was measured at a depth of 7.5 m,[21] which was 1.1 m deeper than the 6.4-m trapping depth identified in the modeling that established the 133:1 minimum dilution ratio. According to the conservative modeling results, dilution levels would be expected to be substantially less than 133:1 at that depth level. Instead, the higher dilutions measured during the mid-depth tow indicate that the diffuser structure was dispersing the effluent far more efficiently than predicted by the modeling, even shortly after discharge and well before the completion of the initial dilution process.

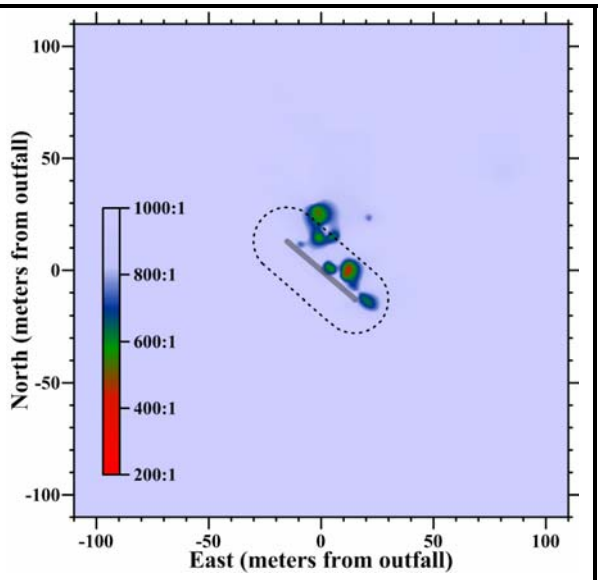

Figure 10. Mid-Depth Plume Dilution Computed from Salinity Anomalies in Figure 8b

As the buoyant plume ascended through the water column and spread toward the northeast by the prevailing current, turbulent mixing continued to dilute the wastewater. Accordingly, salinity data collected during the shallow tow demonstrated that the wastewater had been diluted by at least 534-fold by the time the dilute wastewater rose and additional 3.5 m to a depth level of 4.0 m (Figure 11).

[20] Wastewater samples have an average salinity of 0.995‰.

[21] During this portion of the second mid-depth transect, the CTD was tracking at a slightly shallower depth than the average 8.2 m reported for the entire tow.

Overall, the dilution computations show that, during the March 2016 survey, the outfall was performing better than designed and was rapidly diluting effluent more than 240-fold almost immediately after discharge, and well before completion of the initial-dilution process. As the initial dilution process was nearing completion, effluent had been diluted at least 534-fold, easily exceeding the 133:1 critical initial dilution used to establish end-of-pipe permit limitations on contaminant concentrations within wastewater discharged from the MBCSD treatment plant. This demonstrates that, during the March 2016 survey, the COP receiving-water objectives were being met by the limits on chemical concentrations within discharged wastewater that are promulgated by the NPDES discharge permit issued to the MBCSD.

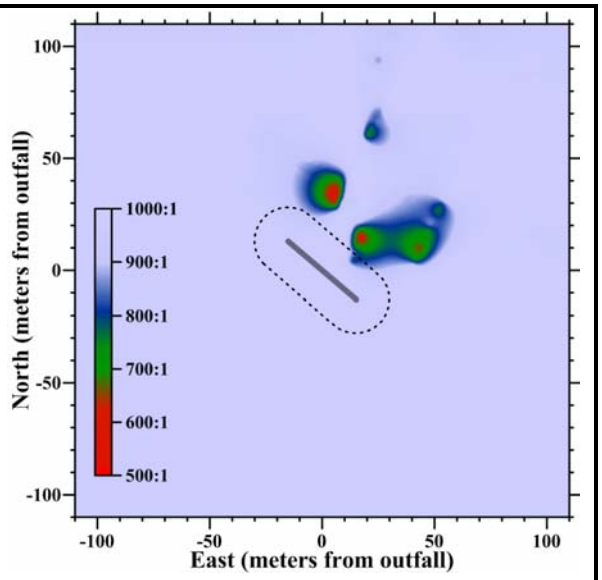

Figure 11. Shallow Plume Dilution Computed from Salinity Anomalies in Figure 9b

COMPLIANCE

This section evaluates compliance with the water-quality limitations listed in the NPDES permit (Table 6). The limits themselves are based on criteria in the COP, the Central Coast Basin Plan, and other state and federal policies that were designed to protect marine life and beneficial uses of ocean waters. Because the limits only pertain to changes in water properties that are caused by the presence of wastewater constituents beyond the ZID, instrumental measurements undergo a series of screening procedures prior to numeric comparison with the permit thresholds. Specifically, the quantitative analyses described in this section focus on water-property excursions caused by the presence of wastewater constituents beyond the ZID, whose amplitudes can be reliably discerned against the backdrop of ambient fluctuations. A detailed understanding of ambient seawater properties, and their natural variability within the region surrounding the outfall, is therefore an integral part of the compliance evaluation presented in this section.

Table 6. Permit Provisions Addressed by the Offshore Receiving-Water Surveys

Limit #	Limit
P1	Floating particles or oil and grease to be visible on the ocean surface
P2	Aesthetically undesirable discoloration of the ocean surface
P3	Temperature of the receiving water to adversely affect beneficial uses
P4	Significant reduction in the transmittance of natural light at any point outside the ZID
P5	The DO concentration outside the zone of initial dilution to fall below 5.0 mg/L or to be depressed more than 10% from that which occurs naturally
P6	The pH outside the zone of initial dilution to be depressed below 7.0, raised above 8.3, or changed more than 0.2 units from that which occurs naturally

The results of these analyses of the March 2016 data demonstrate that the MBCSD discharge complied with the NPDES discharge permit. Moreover, although observations within the ZID are not subject to compliance evaluations, they met the prescribed limits because actual dilution levels routinely exceeded the conservative design specifications assumed in the discharge permit. Thus, the quantitative evaluation described in this section documents an outfall and treatment process that was performing at a high level during the March 2016 survey.

Permit Provisions

The offshore receiving-water surveys are designed to assess compliance with objectives dealing with undesirable alterations to six physical and chemical characteristics of seawater. Specifically, the permit states that wastewater constituents within the discharge shall not cause the limits listed in Table 6 to be exceeded.

The first two receiving-water limits, P1 and P2, rely on qualitative visual observations for compliance evaluation. Compliance was demonstrated during the March 2016 survey through visual inspection of the sea surface that found an absence of floating wastewater materials, oil, grease, and discoloration of the sea surface.

Compliance with the remaining four receiving-water limitations is quantitatively evaluated through a comparison between instrumental measurements and numerical limits listed in the NPDES permit. For example, in P5 and P6, the fixed numeric limits on absolute values of DO (>5 mg/L) and pH (7.0 to 8.3) can be directly compared with field measurements within the dilute wastewater plume beyond the ZID. However, both P5 and P6 also contain narrative limits, which originate in the COP, and define unacceptable water-quality impacts in terms of "*significant*" excursions beyond those that occur "*naturally*." Quantitative evaluation of these limits requires a further comparison of field measurements with numerical thresholds that reflect the natural variation in transmissivity, DO, and pH within the receiving waters surrounding the outfall.

As described previously, natural variation in seawater properties can result from a variety of oceanographic processes. These processes establish the range in ambient seawater properties caused by natural spatial variation within the survey region at a given time (e.g., vertical stratification), and by temporal variations caused by seasonal and interannual influences (e.g., El Niño and La Niña). Of particular interest are upwelling and downwelling processes that not only determine average properties at a given time, but also the degree of water-column stratification, or spatial variability, present during any given survey.

Screening of Measurements

Evaluating whether any of the 11,551 CTD measurements collected during the March 2016 survey exceeded a permit limit can be a complex process. For example, although apparently significant excursions in an individual seawater property may be related to the presence of wastewater constituents, they may also result from instrumental errors, natural processes, entrainment of ambient bottom waters in the rising effluent plume, statistical uncertainty, ongoing initial mixing within and beyond the ZID, or other anthropogenic influences (e.g., dredging discharges or oil spills).

Because of this complexity, measurements were first screened to determine whether numerical limits on individual seawater properties apply (Table 7). The screening procedure sequentially applies three questions to restrict attention to: 1) the oceanic area where permit provisions pertain; 2) changes due to the presence of wastewater particulates; and 3) changes large enough to be reliably detected against the backdrop of natural variation. The measurements that remain after completing the screening process can then be compared with Basin-Plan numerical limits and COP allowances.

Table 7. Receiving-Water Measurements Screened for Compliance Evaluation

Topic Addressed	Screening Question	Answer No	Answer Yes[22]	*Parameter*
Location	1. Was the measurement collected beyond the 15.2-m ZID boundary where modeling assumes that initial dilution is complete?	*1,723*	*9,828*	All
Wastewater Constituents	2. Did the beyond-ZID measurement coincide with a quantifiable salinity anomaly (≤550:1 dilution level) indicating the presence of detectable wastewater constituents?	*9,794*	*34*	All
Natural Variation	3. Did seawater properties associated with the wastewater measurements depart significantly from the expected range in ambient seawater properties at the time of the survey?	*34*	*0*	Temperature
		12	*22*	Transmissivity
		34	*0*	DO
		34	*0*	pH

The following subsection provides additional lines-of-evidence that demonstrate compliance with numerical permit limits independent of the screening process. The rationale for identifying observations suitable for further compliance analysis is presented in the following description of the three screening steps.

1. Measurement Location: The COP states that compliance with its receiving-water objectives "*shall be determined from samples collected at stations representative of the area within the waste field where initial dilution is completed.*" Initial dilution includes the mixing that occurs from the turbulence associated with both the ejection jet, and the buoyant plume's subsequent ascent through the water column.

Although currents often transport the plume well beyond the ZID before the initial dilution process is complete, the COP states that dilution estimates shall be based on "*the assumption that no currents, of sufficient strength to influence the initial dilution process, flow across the discharge structure.*" Because of this, the regulatory mixing distance, which is equal to the 15.2-m water depth of the discharge, provides a conservative boundary to screen receiving-water data for subsequent compliance evaluation. Application of this initial screening question to the March 2016 dataset eliminated 1,723 of the original 11,551 receiving-water observations from further consideration because they were collected within the ZID (Table 7, Question 1). The remaining 9,828 observations were carried forward in the screening analysis.

2. Presence of Wastewater Constituents: The MBCSD discharge permit restricts application of the numerical receiving-water limits to excursions caused by the presence of wastewater constituents. This confines the compliance analysis to changes caused "*as the result of the discharge of waste*," as specified in the COP, rather than anomalies that arise from the upward movement of ambient seawater entrained in the effluent plume. Analyses conducted on quarterly receiving-water surveys over the last decade have

[22] Number of remaining CTD observations of potential compliance interest based on this screening question

demonstrated that the direct influence of dilute wastewater is almost never observed in any seawater property other than salinity, except very close (<1 m) to a diffuser port and within its ejection jet.

In fact, negative salinity anomalies are the only consistent indicator of the presence of wastewater constituents within receiving waters. Wastewater salinity is negligible compared to that of the receiving seawater, so the presence of a distinct salinity minimum provides *de facto* evidence of the presence of wastewater constituents. Because of the large contrast between the nearly fresh wastewater and the salty receiving water, salinity provides a powerful tracer of dilute wastewater that is unrivaled by other seawater properties. Other properties do not exhibit such a large contrast and, as such, their wastewater signatures dissipate rapidly upon discharge with very little mixing. Wastewater's lack of salinity, however, provides a definitive tracer that allows the presence of effluent constituents to be identified even after dilution many times greater than the 133-fold critical initial dilution assumed in the discharge permit.

As described in the previous section, wastewater-induced reductions in salinity can be used to determine the amount of dilution achieved by initial mixing. Based on statistical analyses of the natural variability in salinity readings measured near the outfall over a five-year period between 2004 and 2008, the smallest reduction in salinity that can be reliability detected within receiving waters is 0.062‰. This represents a dilution level of 542-fold in Equation 2. Salinity reductions that are smaller than 0.062‰ cannot be reliably discerned against the backdrop of natural variation and would not result in discernible changes in other seawater properties. Eliminating those measurements from further evaluation restricts attention to excursions in temperature, light transmittance, DO, and pH that are potentially related to the presence of wastewater constituents.

As discussed previously, the lowest salinities measured during the March survey were recorded very close to the diffuser structure during the first part of the mid-depth tow survey. Somewhat higher salinities associated with more dilute portions of the plume were measured beyond the northern boundary of the ZID during subsequent transects of the mid-depth tow. Thirty-four of the salinity reductions measured beyond the ZID corresponded to dilutions less than 550:1 (Table 7). The remaining 9,794 observations that were measured outside the ZID during the March 2016 survey did not have salinity reductions that were greater than the 0.062‰ plume-detection threshold.

3. Natural Variation: An integral part of the compliance analysis is determining whether a particular anomalous measurement resulted from the presence of wastewater constituents, or whether it simply became apparent because ambient seawater was relocated (upward) by the plume. If the measurement does not significantly depart from the natural range in ambient seawater properties at the time of the survey, then it is difficult to ascribe the departure to the presence of wastewater constituents. Thus, quantifying the natural variability around the outfall at the time of the survey is necessary for determining whether a particular observation warrants comparison with the numeric permit limits.

A statistical analysis of receiving-water data collected around the outfall was used to establish the range in natural conditions surrounding the outfall (first three data columns of Table 8). These ambient-variability ranges were used to identify significant departures from natural conditions that could be indicative of adverse discharge-related effects on water quality. The same five-year database used to establish the within-survey salinity variation discussed previously, was also used to establish one-sided 95% confidence bounds on transmissivity (-10.2%), temperature (+0.82°C), DO (-1.38 mg/L), and pH (± 0.094). These were combined with 95th percentiles determined from the March 2016 ambient seawater data, to establish time-specific natural-variability thresholds in a manner analogous to COP Appendix VI. The percentiles were determined from March 2016 vertical profile data collected at Stations RW5 and RW6, thereby excluding measurements potentially affected by the discharge.

Table 8. Compliance Thresholds

Water Quality Property	95% Confidence Bound[23]	95th Percentile[24,25]	Natural Variability Threshold[26]	COP Allowance[27]	Basin Plan Limit[28]	Extremum[29]
Temperature (ºC)	0.82	12.52	>13.34	—	—	≤12.54
Transmissivity (%)	-10.2	67.3	<57.1	—	—	≥39.4
DO (mg/L)	-1.38	5.64	<4.26	<3.83	<5.00	≥5.61
pH (minimum)	-0.094	7.896	<7.802	<7.602	<7.000	≥7.888
pH (maximum)	0.094	7.942	>8.036	>8.236	>8.300	≤7.949

Temperature, pH, and DO concentrations associated with the 34 remaining measurements of potential compliance interest were all well within their respective ranges of natural variability (Table 7, Question 3). As such, the screening process unequivocally eliminated these measurements from further consideration. In fact, all of the documented excursions in these properties were the result of physical processes unrelated to the presence of wastewater constituents, namely, entrainment of near-bottom seawater within the rising effluent plume.

As described previously, anomalies in seawater properties clearly delineated the plume, but those entrainment-generated excursions were not caused by the presence of wastewater constituents. During periods when the water column is even moderately stratified, as it was during the March 2016 survey, ambient seawater properties near the seafloor differ from those within the rest of the water column, and their juxtaposition within the rising effluent plume appears as lateral anomalies within the upper water column. Regardless, if the presence of wastewater particulates had contributed to the measured decreases in DO and pH, their influence would still have been well within the natural range of the ambient seawater properties at the time of the survey. Consequently, their influence on water quality would not be considered environmentally significant.

Transmissivity Measurements of Compliance Interest

Because of the high performance of the treatment process and diffuser system, the screening procedure described above usually eliminates all the measurements collected in a given survey from further

[23] The one-sided confidence bound is used to measure the ability to reliably estimate percentiles within surveys as a whole. They were determined from an analysis of the variability in ambient water-quality data collected during 20 quarterly surveys conducted between 2004 and 2008. Although water-quality observations potentially affected by the presence of wastewater constituents were excluded from the analysis, more than 9,200 remaining observations for each of the six seawater properties accurately quantified the inherent uncertainty in defining the range in natural conditions.

[24] The COP (Appendix I, Page 27, SWRCB 2005) defines a "*significant*" difference as "*a statistically significant difference in the means of two distributions of sampling results at the 95% confidence level*." Accordingly, COP effluent analyses (Step 9 in Appendix VI, Page 42, Ibid.) are based "*the one-sided, upper 95% confidence bound for the 95th percentile*."

[25] The 95th-percentile quantifies natural variability in seawater properties during the March 2016 survey, and was determined from vertical-profiles data unaffected by the discharge.

[26] Thresholds represent limits on wastewater-induced changes to receiving-water properties that significantly exceed natural conditions as specified in the discharge permit and COP. They are determined from the sum of columns to the left and are specific to the March 2016 survey. They do not include the COP allowances specified in the column to the right.

[27] The discharge permit, in accordance with the COP, allows excursions in seawater properties that depart from natural conditions by specified amounts. DO cannot be "*depressed more than 10% from that which occurs naturally*," and pH cannot be "*changed more than 0.2 units from that which occurs naturally.*"

[28] Permit limits P5 and P6 (Table 6) include specific numerical values promulgated in the RWQCB Basin Plan (1994) in addition to changes relative to natural conditions specified in the COP. The Basin Plan upper-bound pH objective for ocean waters is 8.5, but a more-stringent upper-bound objective of 8.3, which applies to individual beneficial uses, was implemented in the MBCSD discharge permit.

[29] Maximum or minimum value measured during the March 2016 survey, regardless of location within or beyond the ZID

consideration in the compliance analysis. However, in a highly unusual circumstance, 22 transmissivity observations from the March 2016 survey were identified for further compliance analysis (Table 7, Question 3). While their identification illustrates the efficacy of the screening process, a more in-depth examination demonstrates why they were selected for further consideration. In fact, they were an artifact of the turbid BNL, whose transient presence was not captured by the vertical profiles used to establish ranges in natural variability.

Usually, when a turbid BNL is present, the vertical profiles capture the sharp reduction in transmissivity immediately above the seafloor. These large declines then factor into the natural variability threshold for transmissivity listed in Table 8. As a result, when naturally turbid seawater is entrained within the rising effluent plume, the resulting reductions in transmissivity within the plume in the upper water column are not flagged as below the natural variability range at the time of the survey.

However, during the March 2016 survey, BNL turbidity, which was entrained within the plume and encountered during the mid-depth tows, was not present later, when the vertical profiling was conducted. As a result, the lower bound of ambient transmissivity threshold (57.1% in Table 8) was well above the lowest transmissivities (39.4%) measured within the plume during the mid-depth tows. During profiling, the lowest transmissivity measured within the plume shortly after discharge remained above 70%. This includes transmissivity measurements collected within the low-salinity plume signature that was encountered shortly after discharge at 14.5m (Figure 7c). Clearly, the low turbidity associated with a BNL was not present when vertical profiling was conducted; otherwise, the transmissivity measured within this plume encounter would have been comparable to those of the mid-depth tow. Similarly, if the effluent discharged at the time of the survey was unusually turbid, and contributed to the decreased transmissivities observed during the mid-depth tows, then the plume encountered during vertical profiling at Station RW3 would have also exhibited markedly lower transmissivities.

For the reasons described below, the 22 reduced-transmissivity measurements identified in the screening process do not constitute an exception to the Permit Requirement P4 limiting reductions *in the transmittance of natural light* (Table 6). First, they were measured below euphotic zone; namely, the 7-m maximum depth of natural light penetration determined from Secchi depth measurements. Second, suspended solids concentration measured within effluent samples onshore at the time of the survey were too small to cause such a reduction in plume transmissivity after accounting for dilution.

Other Lines of Evidence

Several additional lines of evidence further support the conclusion that all the CTD measurements collected during the March 2016 survey complied with permit limits P3 through P6 in Table 6. In combination, these lines of evidence provide the "best explanation" of the origin and significance of individual measurements using abductive inference (Suter 2007). This process, which has been used to implement sediment-quality guidelines for California estuaries (SWRCB 2009), emphasizes a pattern of reasoning that accounts for both discrepancies and concurrences among multiple lines of evidence. A best explanation approach serves to limit the uncertainty associated with each individual CTD measurement, and to provide a more robust compliance assessment. Together, these lines of evidence significantly strengthen the conclusion that the discharge fully complied with the permit at the time of the March 2016 survey.

Insignificant Thermal Impact: Although there are no explicit numerical objectives for discharge-related increases in temperature, a numerical limit can be established for thermal excursions that is based on the requirement that they not adversely affect beneficial uses (P3 in Table 6). Increases in temperature caused by the discharge of warm wastewater constituents could be deemed to affect beneficial uses adversely if they exceeded the natural temperature range observed at the time of the survey (i.e. exceeded 13.34°C in

Table 8). However, none of the 11,551 CTD measurements collected during the March 2016 survey exceeded 12.54°C (last column in Table 8). Additionally, as mentioned previously, because the effluent entrained cooler bottom water shortly after discharge, the rising plume actually exhibited a lower temperature than most of the surrounding seawater (Figures 8a and 9a).

Full Ambient Light Penetration: As with temperature, there are no explicit numerical objectives for discharge-related decreases in transmissivity. However, the COP narrative objective (P4) limiting significant reductions in the transmission of natural light can also be translated into a numerical objective. Specifically, because the COP does not specify an allowance beyond natural conditions, the same threshold on ambient transmissivity variations listed in Table 8 can be interpreted to constitute a numerical limit. However, the 22 transmissivity measurements collected beyond the ZID during the March 2016 survey that fell below the 57.1% minimum compliance threshold, were located beneath the maximum depth of natural light penetration. The base of the euphotic zone, which is considered the limit of maximum light penetration, is defined as twice the Secchi depth. The maximum Secchi depth measured during the March 2016 survey was 3.5 m (Table 4), indicating that the euphotic zone was limited to 7 m. All 22 of the anomalously low transmissivity measurements were collected at greater depth. Thus, even if wastewater particulates contributed to the reduction in transmissivity within the 22 measurements identified in the screening process, they would have had no impact on natural light penetration.

Directional Offset: Analysis of the directional offset of CTD measurements is useful because wastewater and receiving-seawater properties vary from one another in several predictable ways. For example, upon discharge, wastewater is fresher, warmer, and lighter than the ambient receiving waters of Estero Bay. Under most conditions, wastewater is also more turbid than the receiving waters. As such, the presence of wastewater constituents will reduce the salinity, density, and transmissivity of the receiving seawater (negative offset), while temperature will be increased (positive offset). Therefore, as discussed previously, the reduced temperatures observed in conjunction with the effluent plume (Figures 8a and 9a) could not have been generated by the presence of warmer wastewater constituents.

Insignificant Wastewater Particulate Loads: Another independent line of evidence demonstrates that the discharge of wastewater particulates could not have contributed materially to turbidity within the dilute effluent plume. The suspended-solids concentration measured onshore, within the effluent, and immediately prior to discharge from the WWTP on 17 March 2016 was 22 mg/L. After dilution by 240-fold, the effluent suspended-solids concentration would have the reduced ambient transmissivity by only 2.2% within the plume. This small potential decrease in transmissivity was insignificant compared to the naturally occurring 20% reduction in transmissivity that originated within the transient BNL and became apparent during the mid-depth tow.

Similarly, the MBCSD discharge could not have contributed materially to the observed DO fluctuations. The MBCSD treatment process routinely removes 80% or more of the organic material, as demonstrated by the low, 52-mg/L BOD measured within the plant's effluent four days after the survey. That small amount of BOD would have induced a DO depression of no more than 0.022 mg/L after dilution (MRS 2002). In fact, in the absence of tangible BOD influence, wastewater discharge would actually be expected to increase DO within subsurface receiving waters, rather than decrease it. This is because effluent is oxygenated by recent contact with the atmosphere during the treatment process, whereas receiving waters at depth are typically depleted in DO due to the lack of atmospheric equilibration within the deep offshore watermass.

COP Allowances: The COP does not explicitly require that wastewater-induced changes remain within the ranges in natural variation listed in the third data column of Table 8, even though these ranges were conservatively used in the data screening process described in previous subsections. Consideration of

these COP allowances in the receiving-water limits provides an additional level of confidence in the compliance evaluation.

For pH, the COP and the discharge permit allow changes up to 0.2 pH units from natural conditions, bringing the minimum allowed pH down to 7.602 during the March 2016 survey (fourth data column of Table 8). This limiting value is significantly less than the lowest pH measurement of 7.888 recorded during the March 2016 survey (last column of Table 8). Similarly, the lowest DO concentration measured during the survey (5.61 mg/L) was well above both the lower range in natural variation (4.26 mg/L) and the 10% compliance threshold promulgated by the COP (3.83 mg/L).

Excursions remained within the fixed Basin-Plan Limits: Permit provisions P5 and P6 (Table 6) combine receiving-water objectives from both the COP and the Basin Plan with regard to DO and pH limitations. As described previously, the COP requires that DO concentrations outside the ZID not be depressed more than 10% from that which occurs naturally, and restricts pH measurements to those within 0.2 units of that which occurs naturally. In contrast, the Basin-Plan's fixed numerical limits do not provide specific guidance as to how they might change in response to widespread changes in oceanographic conditions unrelated to the discharge. Specifically, the fixed numerical limits restrict DO concentrations outside the ZID to no less than 5 mg/L (P5 in Table 6), and pH levels to the 7.0-to-8.3 range (P6). All of the measurements complied with the Basin-Plan limits, including the more-restrictive limit on minimum DO.

CONCLUSIONS

The quantitative screening analysis demonstrated that all measurements recorded during the March 2016 survey complied with the receiving-water limitations specified in the NPDES discharge permit. This conclusion was further strengthened by other lines of evidence supporting compliance with the discharge permit. Specifically, although discharge-related changes in seawater properties were observed during the March 2016 survey, the changes were either not of significant magnitude (i.e., they were within the natural range of variability that prevailed at the time of the survey), were measured within the boundary of the ZID where initial mixing is still expected to occur, or were not directly caused by the presence of wastewater constituents within the water column.

Shortly after discharge, and well before the initial dilution process was complete, the effluent was achieving dilution levels in excess of 240-fold, which is well more than the critical dilution levels predicted by design modeling. As the plume ascended through the water column and approached the sea surface near the completion of the initial mixing process, dilution levels exceeded 534-fold. All of the measured dilution levels far exceeded levels that were predicted by modeling and that were incorporated in the discharge permit as limits on contaminant concentrations within effluent prior to discharge. Lastly, all of the auxiliary observations collected during the March 2016 survey demonstrated that the discharge complied with the narrative receiving-water limits in the discharge permit and the COP. Together; these observations demonstrate that the treatment process, diffuser structure, and the outfall continue to surpass design expectations.

REFERENCES

Davis, R.E., J.E. Dufour, G.J. Parks, and M.R. Perkins. 1982. Two Inexpensive Current-Following Drifters. Scripps Institution of Oceanography, University of California, San Diego, La Jolla, California. SIO Reference No. 82-28. December 1982.

Fischer, H.B., E.J. List, R.C.Y. Koh, J. Imberger, and N.H. Brooks. 1979. Mixing in Inland and Coastal Waters. New York: Academic Press, 482 p.

Kuehl, S.A., C.A. Nittrouer, M.A. Allison, L. Ercilio, C. Faria, D.A. Dukat, J.M. Jaeger, T.D. Pacioni, A.G. Figueiredo, and E.C. Underkoffler 1996. Sediment deposition, accumulation, and seabed dynamics in an energetic fine-grained coastal environment. *Continental Shelf Research*, 16: 787-816.

Marine Research Specialists (MRS). 1998. City of Morro Bay and Cayucos Sanitary District, Offshore Monitoring and Reporting Program, Semiannual Benthic Sampling Report, April 1998 Survey. Prepared for the City of Morro Bay, CA. July 1998.

Marine Research Specialists (MRS). 2002. City of Morro Bay and Cayucos Sanitary District, Supplement to the 2002 Renewal Application For Ocean Discharge Under NPDES Permit No. Prepared for the City of Morro Bay and Cayucos Sanitary District, Morro Bay, CA. July 2002.

Marine Research Specialists (MRS). 2011. City of Morro Bay and Cayucos Sanitary District, Offshore Monitoring and Reporting Program, 2010 Annual Report. Prepared for the City of Morro Bay, California. March 2011.

Marine Research Specialists (MRS). 2012. City of Morro Bay and Cayucos Sanitary District, Offshore Monitoring and Reporting Program, 2011 Annual Report. Prepared for the City of Morro Bay, California. March 2012.

Marine Research Specialists (MRS). 2013. City of Morro Bay and Cayucos Sanitary District, Offshore Monitoring and Reporting Program, 2012 Annual Report. Prepared for the City of Morro Bay, California. March 2013.

Marine Research Specialists (MRS). 2014. City of Morro Bay and Cayucos Sanitary District, Offshore Monitoring and Reporting Program, 2013 Annual Report. Prepared for the City of Morro Bay, California. March 2014.

National Academy of Sciences. 1993. Managing Wastewater in Coastal Urban Areas. National Research Council Committee on Wastewater Management for Coastal Urban Areas, Water Science and Technology Board, Commission on Engineering and Technical Systems. 477 pp.

Regional Water Quality Control Board (RWQCB) - Central Coast Region. 1994. Water Quality Control Plan (Basin Plan) Central Coast Region. Available from the RWQCB at 81 Higuera Street, Suite 200, San Luis Obispo, California. 148p. + Appendices.

Regional Water Quality Control Board (RWQCB) - Central Coast Region and the Environmental Protection Agency (USEPA) – Region IX. 1992a. Waste Discharge Requirements (Order No. 92-67) and Authorization to Discharge under the National Pollutant Discharge Elimination System (Permit No. CA0047881) for City of Morro Bay and Cayucos Sanitary District, San Luis Obispo County.

Regional Water Quality Control Board (RWQCB) - Central Coast Region and the Environmental Protection Agency (USEPA) – Region IX. 1992b. Monitoring and Reporting Program No. 92-67 for City of Morro Bay and Cayucos Sanitary District, San Luis Obispo County (Permit No. CA0047881).

Regional Water Quality Control Board (RWQCB) - Central Coast Region and the Environmental Protection Agency (USEPA) – Region IX. 1998a. Waste Discharge Requirements (Order No. 98-15) and National Pollutant Discharge Elimination System (Permit No. CA0047881) for City of Morro Bay and Cayucos Sanitary District, San Luis Obispo County. 11 December 1998.

Regional Water Quality Control Board (RWQCB) - Central Coast Region and the Environmental Protection Agency (USEPA) – Region IX. 1998b. Monitoring and Reporting Program No. 98-15 for City of Morro Bay and Cayucos Sanitary District, San Luis Obispo County. 11 December 1998.

Regional Water Quality Control Board (RWQCB) - Central Coast Region and the Environmental Protection Agency (EPA) – Region IX. 2009. Waste Discharge Requirements (Order No. R2-2008-0065) and National Pollutant Discharge Elimination System (Permit No. CA0047881) for the Morro Bay and Cayucos Wastewater Treatment Plant Discharges to the Pacific Ocean, Morro Bay, San Luis Obispo County. Effective 1 March 2009.

Sea-Bird Electronics, Inc. (SBE) 1989. Calculation of M and B Coefficients for the Sea-Tech Transmissometer. Application Note No. 7, Revised September 1989.

Sea-Bird Electronics, Inc. (SBE) 1992. SBE 12/22/22/20 Dissolved Oxygen Sensor Calibration and Deployment. Application Note No. 12-1, rev B, Revised April 1992.

Southern California Bight Field Methods Committee (SCBFMC). 2002. Field Operation Manual for Marine Water-Column, Benthic, and Trawl monitoring in Southern California. Technical Report 259. Southern California Coastal Water Research Project. Westminster, CA. March 2002.

State Water Resources Control Board (SWRCB). 2005. Water Quality Control Plan, Ocean Waters of California, California Ocean Plan. California Environmental Protection Agency. Effective February 14, 2006.

State Water Resources Control Board (SWRCB). 2009. Water Quality Control Plan for Enclosed Bays and Estuaries – Part 1 Sediment Quality. California Environmental Protection Agency. Effective August 22, 2009. sed_qlty_part1.pdf [Accessed 02/26/10].

Suter II, Glenn, W. 2007. Ecological risk assessment, 2nd edition. U. S. Environmental Protection Agency, Cincinnati, Ohio. CRC.

Tetra Tech. 1992. Technical Review City of Morro Bay, CA Section 201(h) Application for Modification of Secondary Treatment Requirements for a Discharge into Marine Waters. Prepared for the U.S. Environmental Protection Agency, Region IX, San Francisco, CA by Tetra Tech, Inc., Lafayette, CA. February 1992.